PNC TN8410 89-047

Factors Affecting Passive Monitoring of Radon

September 1989

TOKAI WORKS

POWER REACTOR AND NUCLEAR FUEL DEVELOPMENT CORPORATION

Factors Affecting Passive Monitoring of Radon

September 1989

Power Reactor and Nuclear Fuel Development Corporation

PNC TN8410 89-047
September 1989

Factors Affecting Passive Monitoring of Radon

Tomohiro ASANO and Bernd KAHN***

ABSTRACT

In recent years, increasing cancer has been expressed as a possible health hazards associated with long-term exposures to a large population at a low level of radon in the environment. Because radon is ubiquitous nuclide, nation-wide monitoring is necessary to determine lung cancer risk. For such purpose, passive sampling methods with track etch detector or charcoal adsorption collector may have the advantage in lower cost and convenience.

The charcoal adsorption collector is considered in this study. Various factors may significantly affect the charcoal adsorption mechanism on its practical application. Moisture effects are discussed here as having major impact on radon collection by charcoal. Set of equations are presented in this report to describe adsorption of radon including moisture effects.

* Power Reactor and Nuclear Fuel Development Corporation
Tokai-mura, Naka-gun, Ibaraki 319-11, Japan
** Georgia Institute of Technology
Atlanta, GA 30332, U.S.A.

PNC TN8410 89-047
１９８９年　９月

ラドンのパッシヴ・モニタリングに係る影響因子について

浅野　智宏*
Bernd KAHN　**

概　要

近年の肺ガン発生率の増加は、環境中の低レベルのラドンによる長期間の被ばくに起因する潜在的な健康影響がひとつの要因とされており、ラドンは環境中のどこにでも存在する核種であるため、広域モニタリングによる肺ガン・リスクの調査が必要とされている。このため、トラック・エッチ法、チャコール吸着法などによるパッシヴなサンプリング方法が、費用と取扱いの容易さの観点から有用な方法とされている。

本報告書では、チャコール吸着によるサンプラーをとりあげ、実際の適用においてチャコールへの吸着メカニズムに影響する因子について検討した。特にラドンのチャコールへの吸着に最も影響を及ぼす因子として、空気中水分の影響について検討した。検討結果は、水分の影響を考慮したラドンの吸着式としてとりまとめた。

＊　動力炉・核燃料開発事業団　東海事業所　安全管理部
＊＊ジョージア工科大学　保健物理学科教授

C O N T E N T S

1. INTRODUCTION

The relationship between illness and ore mining in central Europe was recognized in early 16th century, and lung cancer was identified as the principal disease of these miners in 19th century. Radon and its progeny were involved as causative agents for miners in the same century. In recent years, increasing cancer has been expressed as a possible health hazards associated with long-term exposures over a large population to a lower level of radon in the environment.

Although there may be uncertainties about the risk of radon, epidemiological studies were conducted by several scientific committees (UNS77, NAS84, NCRP84, ICRP87, NAS88). Recognition of the risk of radon, U.S. Environmental Protection Agency (EPA) suggested that approximately 20,000 deaths in 1987 in the United States was due to environmental concentration of radon (Pus88). NCRP also suggested that 55 % of the total average dose equivalent in the US population, i.e., most contributor to total dose, is due to radon in the environment (NCRP87). Because the radon is one of the ubiquitous nuclide, nation wide survey is necessary to determine lung cancer risk.

Various methods for the measurement of environmental concentration of radon have been developed and demonstrated. For the purpose of nation wide monitoring, passive sampling methods such as track etch and charcoal adsorption collector may have the most advantage in its lower cost and convenience.

Charcoal, however, is an excellent adsorption of many gases and vapors other than radon. It is known that the quantity of radon adsorbed is reduced as humidity increases (Coh83, Gra84). This problem is usually addressed by determining the mass increase of charcoal during exposure, and using this as a measure of humidity to derive correction.

In chapter 2, previous risk studies of environmental concentrations of radon are reviewed to recognize present status. In chapter 3, various factors affecting charcoal adsorption collector are summarized, and moisture effects on the adsorption of radon on charcoal are discussed here as having major impact on its practical application.

2. RISK ESTIMATE OF RADON

2.1 Radon Dosimetry

Source of radon-222 and its progeny in the atmosphere is the radium-226 which naturally present in various materials such as soil, water and building materials, and which is the fifth daughter of uranium-238. Decay scheme of radon is given in Fig.2-1. Radon-222 decays with a half life of 3.82 day into a series of solid, short-lived radioisotopes. These daughters have no independent existence in the atmosphere. Two of these daughters, polonium-218 and polonium-214, emit alpha particles, which, when emission occurs in the lung, can damage the cells lining. The resulting biological changes can ultimately lead to lung cancer.

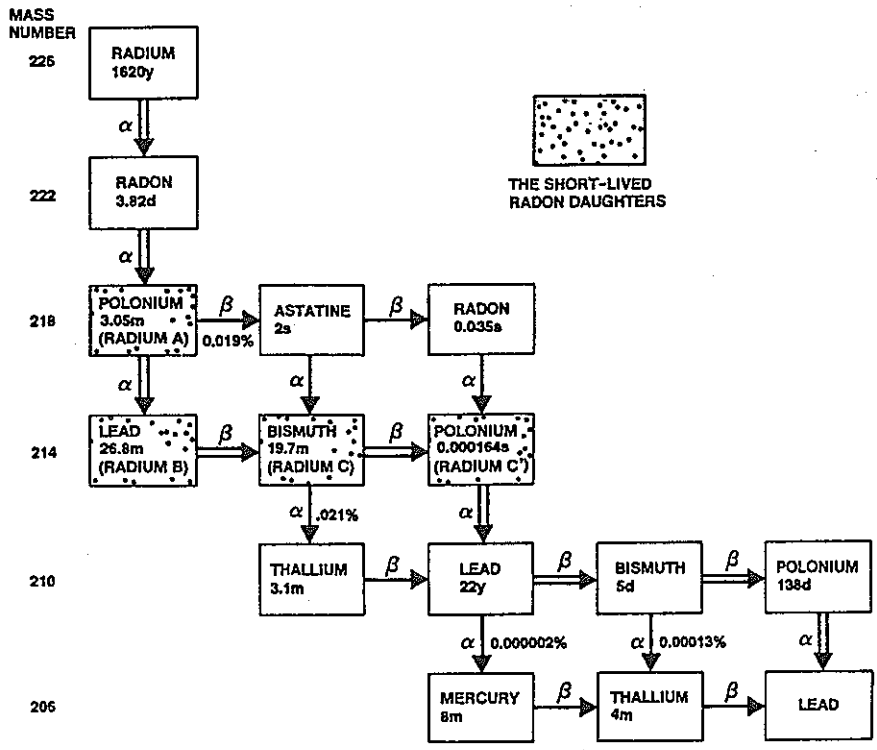

The radon decay chain. An arrow pointing downward indicates a decay by alpha-particle emission; an arrow pointing to the right indicates a decay by beta-particle emission. The historical symbols for the nuclides are in parentheses below the modern symbols. Most of the decays take place along the unbranched chain marked by the double arrows. The negligible percentage of the decays going along the single arrows is shown at critical points. The end of the chain, lead-206, is stable, not radioactive. Half-lives are shown for each isotope with s = seconds, m = minutes, d = days, and y = years.

Fig.2-1 Decay Chain of Radon (NAS88)

The major source of radon in the atmosphere is the routine emanation from the radium-226 in the earth's surface. These sources are tabulated in Table 2-1 (NCRP84). The estimated ranges of radon-222 concentration levels from different sources in typical houses are summarized in Table 2-2 (ICRP87). Major contribution to the indoor air concentration of radon is entry from soil. Possible transport mechanism are molecular diffusion and convective flow. Of most importance is believed to be the latter process, which is induced by

Table 2-1 Sources of Global Atmospheric Radon-222 (NCRP84)

Source	Release Rate (Ci/y)
Emanation from Soil	2×10^{9}
Ground Water (Potential)	5×10^{8}
Emanation from Ocean	3×10^{7}
Phosphate Residues	3×10^{6}
Uranium Tailing Piles	2×10^{6}
Coal Residues	2×10^{4}
Natural Gas	1×10^{4}
Coal Combustion	9×10^{2}
Human Exhalation	1×10^{1}

Table 2-2 Concentration of Rn-222 in indoor air from different sources (ICRP87)

Source	Indoor Concentration (Bq/m^3)	
	Estimated mean	Range of variation
Building materials		
brick or concrete houses	3 - 30	0.7 - 100
wooden houses	< 1	0.03 - 2
Soil	2 - 60	0.5 - 500
Outdoor air	3 - 7	1 - 10
Other sources (water, natural gas)	< 0.1	0.01 - (10)
All sources	10 - 100	2 - 500

pressure differences between soil and indoor air. Entry rate from soil depends strongly on the permeability of the underlying soil and of the understructure of the house.

Because of their wide distribution, radon and its progeny are a major source of exposure for the general public as well as for workers in mines. In most of the cases, the concentration of radon daughters is measured in working levels (WL) and cumulative exposures over time are measured in working-level months (WLM). These quantities are described as follows (NAS88) ;

> *" The working level (WL) is defined as any combination of the short-lived radon daughters in 1 liter of air that results in the ultimate release of 1.3 x 10^5 MeV of potential alpha energy. This is approximately the amount of alpha energy emitted by the short-half-life daughters in equilibrium with 100 pCi of radon. Exposures of a miner to this concentration for a working month of 170 hr (or twice this concentration for half as long, etc.) is defined as a working-level-month (WLM). Note that the cumulative exposure in WLM is the sum of the products of radon-progeny concentrations and the times of exposure. For historical reasons, time is quantified into blocks of 170 hr when the concentration is expressed in WL. This can lead to confusion in domestic environments, because a 30-day month is 720 hr. Exposures to 1 WL for 720 hr results in a cumulative exposure of 4.235 WLM. Home occupancy for 12 hr/day at 1 WL would result in a cumulative exposure of about 2.12 WLM per month of occupancy. "*

The relationship between exposure and dose to target cells and tissues in the respiratory tract is complex and depends on both biological and nonbiological factors. Factors influencing the dosimetry of radon daughter include physical characteristics of the inhaled air, breathing patterns, smoking habit, and the biological characteristics of the lung. In most cases epidemiological studies on miners are extrapolated to general populations.

2.2 Risk Studies of Radon

(1) ICRP Task Group

An ICRP Task Group report, ICRP publication 50, provides comprehensive information on risk models both relative and absolute(ICRP87). The model itself and related parameters are discussed in the report.

As given in the report, Brown performed a survey on the mean residence probability of individuals in private houses, other buildings, and outdoors as a function of time of day (Bro83). Based on his report, ICRP Task Group recommended the following reference relationship for the evaluation of the annual exposure to Rn-222 and Rn-220 daughters ;

$$E = 6000\ Cih + 1500\ Cie + 1000\ Co \qquad (2\text{-}1)$$

Where,

E : Equilibrium-equivalent concentration (Bq h/m^3)
Cih : Equilibrium-equivalent concentration in the air of private homes (Bq/m^3)
Cie : Equilibrium-equivalent concentration in other building (Bq/m^3)
Co : Equilibrium-equivalent concentration in outdoor air (Bq/m^3)

The values of 6000, 1500, 1000 are mean residence times in hours per year in private homes, other building, and outdoor. For a person not engaged in employment outside the house, mean residence time in homes, 6000 hrs, is about 20 % higher, but the residence time in other building is correspondingly reduced. Using typical concentration values, about 75 % of the total exposure is associated with private homes, and only 5 % is due to outdoor exposure.

The Task Group also suggests reference values of the dose. According to the analysis, the effective dose equivalent to adults due to equilibrium-equivalent concentration of Rn-222 is given by ;

$$He = 0.061\ Cih + 0.016\ Cie + 0.014\ Co \qquad (2\text{-}2)$$

For children, the dosimetric models indicate a bronchial dose per unit exposure which is up to a factor of 2 higher than for adults. In NEA-report, an average factor of 1.5 for the age group from 0 - 10 years is suggested (NEA83).

The Task Group considered two different concepts of risk evaluation models ; relative and absolute. The basic quantity employed in the relative risk projection model is the age-specific lung cancer mortality rate. This quantity defines the probability per unit time of dying from lung cancer at a given age after having reached this age. Using this quantity, the integral risk of lung cancer such as individual lifetime risk of lung cancer, radiation-induced lung cancer frequency among the general populations, and corresponding loss of life expectancy from radiation-induced lung cancer can be expressed. Available epidemiological data on lung cancer for underground miners are corrected for the populations. Relative risk coefficients for indoor exposure to Rn-222 and its daughters are given in Table 2-3.

The absolute risk projection model has been mainly considered before studies by the ICRP Task Group. The NCRP used the absolute risk model (NCRP84). For this reason,

Table 2-3 Estimated mean values of the relative excess risk coefficient (ICRP87)

	Relative excess risk coefficient	
Age at exposure	$(Bq\ h/m^3)^{-1}$	WLM^{-1}
0 - 20	3.0×10^{-8}	0.019
<20	1.0×10^{-8}	0.0064

absolute risk model is also discussed in the ICRP Publication. Contrary to the relative risk projection model, the absolute risk model presumes no correlation between the appearance rate of lung cancer and the normal, strongly age-dependent, lung cancer rate. The previous studies yield a lifetime risk of 0.1 - 0.3 % at the given reference exposure conditions. This correspond to an age-average risk to exposure ratio ;

$$Rr/E = (1 \sim 3)\ 10^{-10} \quad \text{(per Bq h/m}^3\text{)}$$
$$= (0.6 \sim 1.8)\ 10^{-4} \quad \text{(per WLM)}$$

for indoor exposure to radon daughters. Where, Rr is individual lifetime risk of lung cancer and E is cumulative exposure time.

In Table 2-4, best estimates from the absolute risk models of the attributable lifetime risk of lung cancer for chronic indoor exposure to radon-222 daughters are compared with the sex-averaged risk value resulting from the relative risk model. The value from the relative risk model is about a factor of 1.5 higher than the results of the absolute risk model based on data from radon exposed miners.

Table 2-4 Comparison of Estimate from Different Risk Projection Models (ICRP87)

Type of approach	Lifetime risk Rr for chronic exposure of 10^5 Bq h/m^3 in each year	1 WLM in each year
Relative risk projection		
reference population	0.0026	0.016
non-smoker only	0.0006	0.004
Absolute risk projection		
ICRP study	0.0018	0.011
NCRP model	0.0015	0.0095
dosimetric approach	0.0010	0.0070

(2) EPA

As given in Table 2-5, the reported number of lung cancer deaths in the United States has increased dramatically after 1930. The increase of lung cancers is due to population growth and aging of the population. There might be several sources of error such as erroneously including deaths due to tuberculosis or other diseases of the respiratory system and problems with misdiagnosis. Even after taking such reasons into account, there has clearly been a great increase in lung cancer mortality. Most of this increase is attributable to cigarette smoking. The U.S.Surgeon General estimated that 85 % of all lung cancers are caused by cigarette smoking.

The risk estimate by EPA was derived on the basis of a relative risk model. The incremental risk of a given effect associated with a given exposure is assumed to be linearly proportional to the baseline rate of the effect in the population. In the EPA model, the constant of proportionality (relative risk coefficient) is taken to be independent of age, sex and smoking status.

Table 2-5 U.S.population and lung cancer mortality figures for the period 1930-1980 (Pus88)

Year	Population (millions)	Lung Cancer Deaths		Age Standardized Rates (10^{-5}/y)	
		Male	Female	Male	Female
1930	123.2	1,803	1,008	3.29	1.93
1940	132.2	6,035	2,012	9.10	3.06
1950	151.3	14,545	3,169	18.0	3.70
1960	179.3	31,242	5,158	31.9	4.70
1970	203.2	52,793	12,360	47.0	9.42
1980	226.5	75,528	28,304	56.1	17.4

Puskin and Yang employed the range of relative risk coefficients of 0.3 - 3.6 % per WLM to calculate lung cancer mortality rate (Pus88). The EPA estimates Rn-induced lung cancers on the basis of a relative risk model, assuming a 10-y minimum latency period and a 2 % per WLM relative risk coefficient extrapolated from miner studies. In applying the model to the case of indoor exposures of the general public, however, the exposure value is adjusted, on an age-specific basis, to correct for differences in lung morphology and difference of breathing rates between miners and members of the public. The net effect of this adjustment is to reduce by about 40 % the calculated excess cancers induced by continuous lifetime exposures to indoor radon. This yields relative risk coefficient of 1.2 % per WLM. Upper and lower bound estimates are approximated 2.4 % per WLM and 0.6 % per WLM, respectively. The average exposure rate was assumed to be 0.25 WLM per year, corresponding to an assumed average radon daughter level of 0.00646 WL at a 75 occupancy factor. Under such assumptions, the EPA model projects, for 1987, about 19,500 (10,500 - 34,000) radon-induced lung cancer deaths in the United States. This means that about 14 % (8 - 25 %) of all lung cancer deaths are currently attributable to radon.

(3) BEIR IV

The most extensive study of radon risk is provided in the BEIR IV report (NAS88). The BEIR IV committee developed its own risk estimates based on analysis of four of the principal data sets related to lung-cancer occurrence in underground miners. The analysis indicated that the risk of lung-cancer mortality due to radon-daughter exposure was explained best by a model in which the excess relative risk is directly proportional to the cumulative exposure, but modified by the age at which the risk occurs and the length of time since exposure. However, the Committee's model contained risk coefficients that reflect a declining risk over time since exposure (at and after 15 years) and age (at and after 55 years of age) when compared with predictions based on a constant relative risk model.

Indoor radon risks can be estimated with the committee's model based on occupational exposure, but several assumptions are required. For the purpose of risk examination, the committee assumed that the findings in the miners could be extended across the entire life span, that 1 WLM yields an equivalent dose to the respiratory tract in occupational and environmental settings, that cigarette smoking and radon-daughter exposure interact multiplicatively, and that the sex-specific baseline risk of lung cancer is increased multiplicatively by radon daughters for males and females.

The Committee's summary estimate of lifetime risk was 350 lung cancer deaths per 10^6 person-WLM of lifetime exposure for a population containing equal number of males and females.

(4) Summary of Risk Estimates

Estimates of the lifetime risk of lung-cancer mortality due to lifetime exposure to radon and its progeny are summarized in Table 2-6. UNSCEAR, BEIR III and NCRP have radon lung cancer mortality rate on the absolute risk model. The ICRP Task Group discussed relative risk projection and absolute risk projection models. A reference mortality rate given for the absolute risk projection model is shown in Table 2-6. The EPA employed a constant relative risk model, and the BEIR IV Committee a employed time-since-exposure (TSE) relative risk model. Most of the recent studies suggest several hundred deaths per 10^6 person WLM.

Table 2-6 Comparisons of Estimate of Lifetime Risk of Lung-Cancer Mortality due to Lifetime Exposure to Radon Progeny

Risk Study	Excess Lifetime Lung-Cancer Mortality (deaths/10^6 person WLM)
UNSCEAR (1977)	200 - 450
BEIR III (1980)	750
NCRP (1984)	130
EPA (1986)	460
ICRP (1987)	230
BEIR IV (1988)	350

2.3 Risk Comparison with Other Sources of Ionizing Radiation

All members of the public are inevitably exposed to sources of ionizing radiation. The sources are of three general types : natural origin unperturbed by human activities, those of natural origin but affected by human activities and man-made sources. Attempts to quantify all the ionizing radiation exposure to the population in the United States were made by National Council on Radiation Protection and Measurements (NCRP87).

The number of people exposed to these sources, the effective dose equivalent to those exposed, the effective collective dose equivalent and the average effective dose equivalent (He) in the U.S.population are given in Table 2-7. For illustrative purposes, the percent contribution of the various radiation sources to the total effective dose equivalent to the members of the U.S. population are given in Fig.2-2. The contributions to the genetically significant dose (GSD) are listed separately in Table 2-8. These results are for various years within the period 1977-1984, with most of the data being for 1980-1982.

The average annual effective dose equivalent from all sources in the entire U.S.population is obtained by summing the annual collective effective dose equivalents and dividing by 230 million, taken as the U.S.population in 1980. The result is approximately 3.6 mSv annually for all people in the U.S. from all sources, excluding cigarette smoking, i.e., about 0.01 mSv/d.

For the 50 million smokers in US, there is an additional exposure to the lungs from naturally occurring radionuclides in cigarettes. The effective dose equivalent from this source is difficult to estimate. A small segment of the bronchial epithelium appears to receive about 0.16 Sv/y on the average and this is probably dependent on the number of cigarettes smoked.

The GSD is about 1.3 mSv/y from all sources, including a small contribution from consumer products which irradiate the whole body.

The data of Table 2-7 indicate that natural sources make the greatest contribution to the average annual effective dose equivalent for members of the U.S.population. Among these natural sources, radon and radon decay products indoors are the largest contributors to the average annual effective dose equivalent. They make a small contribution to the annual GSD.

Table 2-8 Annual GSD in the U.S.population circa 1980-1982 (NCRP87)

Source	Contributions to GSD (mSv)
Natural sources	
Radon	0.1
Other	0.9
Occupational	~0.006
Nuclear fuel cycle	<0.0005
Consumer products	
Tobacco	-
Other	~0.05
Miscellaneous environmental sources	<0.001
Medical	
Diagnostic x rays	0.2 - 0.3
Nuclear medicine	0.02
Rounded total	~1.3

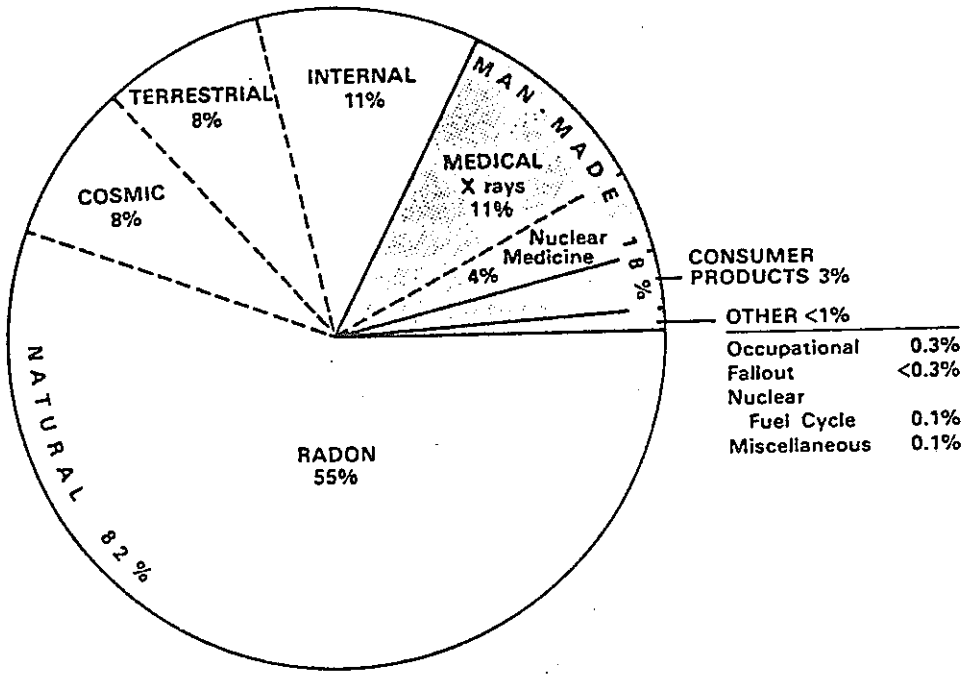

Fig.2-2 Percentage contribution of various radiation sources to the total average effective equivalent in the U.S. population (NCRP87)

Table 2-9 gives published estimates of average individual doses from all sources to the U.K. population by National Radiological Protection Board (NRPB) (Bro83). The values indicate that just under 80 % of the total effective dose equivalent received by the U.K. population comes from natural sources. On average, each person receives an effective dose equivalent of about 0.8 mSv a year from radon decay products out of a total of about 2.4 mSv a year. Although the extent may vary, radon and its progeny are the most important exposure pathway in both countries.

Table 2-9 Average annual effective dose equivalents to the U.K. population from all sources (Bro83)

Source	Average annual effective dose equivalent (μSv in a year)
Cosmic radiation	310
Internal irradiation	370
Terrestrial gamma rays	380
Radon decay products	800
Medical irradiation	500
Fallout	10
Occupational exposures	9
Miscellaneous sources	8
Disposal of radioactive waste	3

3. PASSIVE MONITORING OF RADON BY CHARCOAL

3.1 Indoor Radon Monitoring

As discussed in the previous section, indoor radon is one of the most important source of ionizing radiation for the general public, but depend on locality, radon concentration level and individual behavior.

Nero et al. reviewed published information on monitoring data from U.S. single-family homes (Ner86). Several ways of aggregating data were used to take into account differences in sample selection and season of measurements. The resulting distribution of annual average radon-222 concentrations can be characterized by an arithmetic mean of 56 mBq/l (1.5 pCi/l) and a long tail with 1 to 3 % of homes exceeding 300 mBq/l (8 pCi/l), or by a geometric mean of 33 mBq/l (0.9 pCi/l) and a geometric standard deviation of about 2.8. The standard deviation in the means is 15 %, estimated from the number and variability of the available data sets, but the total uncertainty is larger because data may not be representative. Available dose-response data suggest that the average of 56 mBq/l (1.5 pCi/l) contributes about 0.3 % lifetime risk of lung cancer and that, in the million homes with the highest concentrations, where annual exposures approximate or exceed those received by underground uranium miners, long-term occupants suffer an added lifetime risk of at least 2 %, reaching extraordinary values at the highest concentrations observed.

More nation-wide and detailed investigations on indoor radon concentrations are required to quantify the risk of radon. The techniques developed for measurement of integrated concentration of airborne radon are : the plastic bag method (Sil69), passive environmental radon monitor with TLDs (Geo77), track etch method (Alt81), diffusion barrier charcoal adsorption (DBCA) collector (Coh83, Coh86a, Coh86b), alpha-spectroscopy monitor (Wat86), and electret passive monitor (Kot88). Some of them are too expensive or complicated for nation-wide monitoring, hence, passive

sampling by track etch method and DBCA collector may have advantage in its lower cost and handling convenience. Cohen compared the track etch and charcoal adsorption methods for measurement of indoor radon air concentrations (Coh86b).

The passive charcoal adsorption method depends on diffusion phenomena. Diffusional sampling was developed for the monitoring of organic vapor, and numerous researches has been demonstrated its effectiveness (Ros82, Har87). The DBCA collector developed by Cohen et al. demonstrated its effectiveness for monitoring radon. Charcoal, however, is an excellent adsorbent for many gases other than radon, including water vapor in the air. It is known that the amount of adsorbed gases is reduced as humidity increases.

The purpose of this section is to describe uncertainties involved in the charcoal adsorption sampling, and to discuss moisture effect on the adsorption of radon on charcoal.

3.2 Methodology of Passive Monitoring

3.2.1 Sampling Theory

Contrary to the dynamic samplers, passive samplers do not use an air moving device to transport contaminant to the charcoal surface. Natural forces are used to ensure that a representative amount of contaminant molecules is collected on the charcoal. Two principles are used in sampler design. The first is diffusion from ambient air through the diffusion path to the charcoal surface. The second involves adsorption of contaminant molecules in the charcoal.

(1) Diffusion Sampling

Passive sampling relies on the movement of molecules across the concentration gradient in steady-state conditions and can be defined by Fick's First Law. Fick's Law gives the sampling rate by a passive sampler in terms of the diffusion coefficient and the concentration gradient.

$$dW/dt = - DA\ dC/dx \qquad (3\text{-}1)$$

where,

- dW/dt : Sampling rate (Bq/s or g/s)
- D : Diffusion coefficient (cm^2/sec)
- A : Cross sectional area of diffusion path (cm^2)
- dC/dx : Concentration gradient across diffusion path (Bq/cm^4 or g/cm^4)

Fig.3-1 gives a schematic diagram of a passive sampler, in which the sampling surface consists of a thin layer of adsorbent separated from the ambient air by diffusion path L (Und84). Considering the change in concentration across the diffusion path, equation (3-1) can be written as,

$$dW/dt = AD/L\ (Co - C) \qquad (3\text{-}2)$$

where,

- L : Length of diffusion path (cm)
- Co : Ambient concentration of gases (Bq/cm^3 or g/cm^3)
- C : Concentration of gases at the charcoal surface (Bq/cm^3 or g/cm^3)

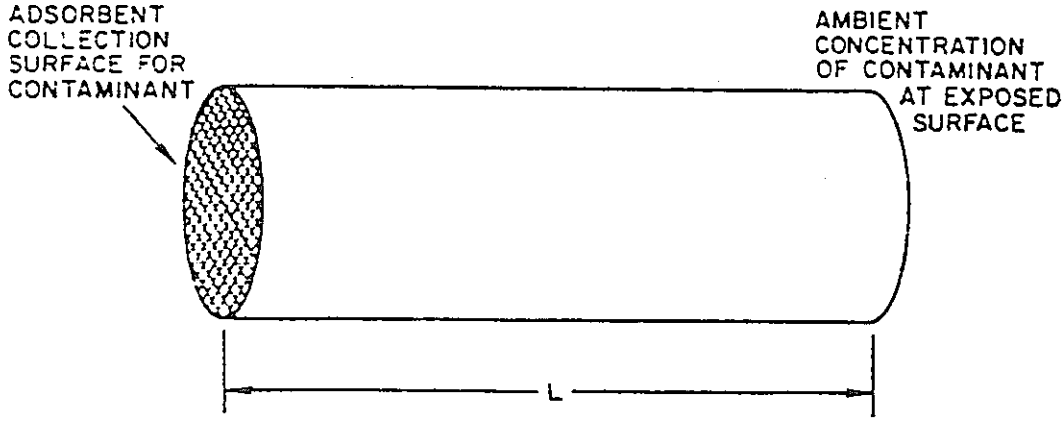

Fig.3-1 Schematic diagram of a passive sampler (Und84)

Equation (3-2) means that the sampling rate is proportional to the concentration difference across the diffusion path, the cross-sectional area of the diffusion path, the diffusion coefficient, and inversely proportional to the length of diffusion path. The unit of AD/L correspond to the sampling flow rate of the dynamic open-end sampler which uses air moving device such as a pump. In this study, an activated charcoal is used as collection medium. If the charcoal is a perfect collection medium, the concentration of gases at the charcoal surface, C, can be assumed to be zero. However, such high sampling efficiency is not expected for charcoal. The adsorption mechanism should be taken into account for the collection of gases.

(2) Linear Adsorption

The adsorption of the charcoal may be due to either weak interactions such as van der Waals force, or chemical interactions (Bru43). Linear and nonlinear adsorption isotherm have been developed and validated through numerous experiments for various gases and vapors.

Assuming that the vapor pressure of the gases at the sampling surface is proportional to the quantity of sampled gases, i.e., assuming a linear isotherm,

$$C = W/km \qquad (3\text{-}3)$$

where,

k : Adsorption coefficient (Bq/g-charcoal per Bq/cm^3-air, or cm^3/g)

m : Mass of charcoal (g)

It is instructive to assume that the ambient concentration of gases in the air is constant during sampling period. Then,

$$dW/dt = AD/L\ (Co - W/km) \qquad (3\text{-}4)$$

Rearranging equation (3-4),

$$dW/(kmCo - W) = ADdt/kmL \qquad (3\text{-}5)$$

Integrating dW and dt over 0 - W and 0 - t, respectively,

$$W = kmCo\ (1-\exp(-ADt/kmL)) \qquad (3-6)$$

Equation (3-6) means that time dependent ingrowth of the adsorbed amount of gases (W) is expressed by exponential term with time constant (AD/kmL) until saturation state (kmCo). Because equation (3-3) assumes equilibrium state for the ambient concentration and adsorbed amount of gases, equation (3-6) must be applied to equilibrium conditions.

The next problem is how to quantify pre-equilibrium state. According to Fick's Second Law, the concentration in charcoal can be expressed by,

$$\partial Cc/\partial t = D\ \partial^2 Cc/\partial x^2 \qquad (3-7)$$

where,

Cc : Concentration of gases in charcoal (Bq/cm^3)

x : Depth of the charcoal bed (cm)

Assuming linear isotherm, the boundary condition at the charcoal surface can be,

$$\text{at } x = 0,\ Cc = k\ \rho\ Ca(t) \qquad (3-8)$$

where, ρ is the density of the charcoal (g/cm^3), and Ca(t) is the concentration of gases in the air (Bq/cm^3). Considering the behavior of a short pulse of gases,

$$Ca(t) = Co\ \tau\ \delta(t) \qquad (3-9)$$

where τ is time of a short pulse and $\delta(t)$ is the delta function which is zero everywhere except at t = 0 and satisfies,

$$\tau(t)\ dt = 1 \qquad (3-10)$$

This gives an integrated exposure, $Ccdt = Co\ \tau$, essentially the same as a concentration Co lasting for a short time τ. Then the boundary condition (3-8) becomes,

$$\text{at } x = 0,\ Cc = A\ \delta(t),\ \text{where } A = k\rho Co\tau \qquad (3-11)$$

The solution of (3-7) with the boundary condition (3-11) is obtained by use of La-place transforms as (Coh83);

$$Cc = Ax/2\sqrt{(\pi\ D\ t^3)}\ \exp(-x^2/4Dt) \qquad (3\text{-}12)$$

According to equation (3-12), the diffusion of gases inside charcoal bed may spread out over a distance of,

$$x = 2\sqrt{Dt} \qquad (3\text{-}13)$$

It is useful to consider a closed-end passive canister. The finite depth x is equivalent to the charcoal bed depth (h) of the canister. When the diffusion front reaches the bottom of the canister, it is reflected from the bottom and the reflected front comes back to the charcoal surface. Then, the traveling distance of the reflected front is twice the charcoal depth (2h). After that, the adsorption of gases can be approximately assumed to be equilibrium. The time to reach equilibrium can be given by,

$$Teq = h^2/D \qquad (3\text{-}14)$$

After Teq, equilibrium equation (3-6) may be used to determine adsorbed amount of gases on the charcoal.

Carrier gases involving air compete with the gas of concern for the adsorption site of the charcoal. At low concentrations of the gases, this competition linearizes their adsorption isotherms by converting their heat of adsorption on very active sites into the lesser value of a heat of displacement. The net results is that, at moderate and low concentrations of gases, the adsorption isotherm is either linear or very nearly linear. At low concentrations, the independence or near independence of the adsorption coefficient on concentration has been substantiated by previous studies (Und80).

(3) Nonlinear Adsorption

A basic concept of the Polanyi theory is that an adsorbate can be characterized by an attractive force field over the microporous surfaces of the adsorbent. The schematic representation of the force field at the adsorption surface is given in Fig.3-2. Polanyi has described these forces by an adsorption potential, which is defined for a point near the surface of the adsorbent, as the work done by the attractive forces in bringing a molecule of a gas to that given point (Dub60). The adsorption potential has its maximum value at the surface of the adsorbent and it decrease to zero at some limiting distance (Bru43, Und87).

The adsorption potential termed in Polanyi potential theory is expressed as (Dub60),

$$\varepsilon = RT \ln(P/Ps) \qquad (3\text{-}15)$$

where,

- ε : Adsorption potential (cal/mol)
- R : Gas constant (1.987 cal/mol/ K)
- T : Temperature (K)
- P : Vapor pressure
- Ps : Saturated vapor pressure

Reucroft assumed the Dubinin-Polanyi (Dubinin-Radushkevich) nonlinear isotherm to describe mixed vapor adsorption mechanism (Reu84). The Dubinin-Polanyi equation is,

$$\ln Wv = \ln Wm - kc\ \varepsilon^2 \qquad (3\text{-}16)$$

where,

- Wv : Volume of adsorbate per gram charcoal (cm^3/g)
- Wm : Maximum pore volume of adsorption space per gram charcoal (cm^3/g)
- kc : Constant related to the pore volume structure of the charcoal (mol^2/cal^2)

Equation (3-16) is also written as,

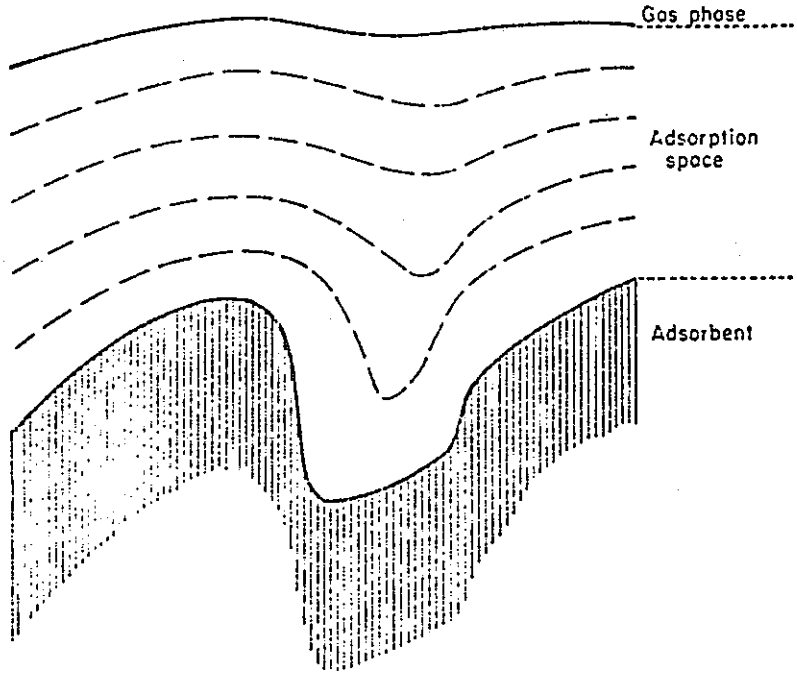

Fig.3-2 Schematic representation of force field at the adsorption surface according to the potential theory (Bru43)

$$Wv = Wm \exp(- kc \varepsilon^2) \qquad (3\text{-}17)$$

Table 3-1 gives equations for three common non-linear isotherms such as Langmuir, Fruendlich and Dubinin-Radushkevich (Dubinin-Polanyi) isotherms. Equation (3-2) can be integrated numerically, if the adsorption isotherm is known. Underhill calculated the sampling efficiency of each isotherm as given in Fig.3-3. The sampling efficiency is the ratio of the sampling rate to the initial (and maximum possible) rate of sampling. Non-dimensionalized time, τ, is defined as given in Table 3-1 for each isotherm. Underhill concluded that the Dubinin-Radushkevich isotherm, commonly seen for adsorption by charcoal, is consistent with high sampling efficiency (Und84). Golovoy and Braslaw demonstrated the Dubinin-Polanyi approximation to determine equilibrium adsorption isotherms of 14 solvents such as n-heptane, n-butanol, and methy isobutyl ketone. Using n-heptane as a reference solvent, they found a mean error of 1.9 % and the maximum error 7.2 % (Gol81).

TABLE 3-1

Dimensionless Equations for the Sampling and Retention of Airborne Vapors by Passive Samplers

Isotherm	Dimensional Isotherm	Nondimensionalized Isotherm	Uptake of Adsorbate	Sampling Efficiency	Retention Efficiency	Definition of Dimensionless Variables for each Isotherm
Linear	$W = kmC$	$w = c$	$r = -\ell n\,(1-w)$	$\dot{w} = 1-w$	$r = -\ell n\,(w)$	$w = \frac{W}{kmC_o}$; $\tau_h = \frac{ADt}{kmL}$
Langmuir	$W = \frac{mbC}{1+aC}$	$w = \frac{c}{1-r+rc}$	$r = wr+(r-1)\ell n(1-w)$	$\dot{w} = \frac{1-w}{1-rw}$	$r = \frac{r(w-1)-\ell n(w)}{1-r}$	$w = \frac{(1+aC_o)W}{mbC_o}$; $r = \frac{aC_o}{1+aC_o}$; $\tau_h = \frac{AD(1+aC_o)t}{mbL}$
Fruendlich	$W = mac^{1/b}$	$w = c^{1/b}$	$r = \sum_{o}^{\infty} \frac{w^{nb+1}}{nb+1}$	$\dot{w} = 1-w^b$	$r = \frac{1-w^{1-b}}{1-b}$	$w = \frac{W}{maC_o^{1/b}}$; $\tau_h = \frac{ABC_o^{1-1/b}t}{maL}$
Dubinin-Radushkevich	$W = m\rho v_o e^{-\frac{BR^2T^2}{\beta^2}\ell n^2(\frac{C}{C_L})}$	$w = e^{b[\ell n^2 a-\ell n^2(ac)]}$	$r = \int_{o}^{w} \frac{dw}{1-c}$	$\dot{w} = 1-c$	$r = \int_{w}^{1} \frac{dw}{c}$	$w = \frac{W}{m\rho v_o} e^{b\ell n^2 a}$; $\tau_h = \frac{ADC_o t}{m\rho v_o L} e^{b\ell n^2 a}$; $a = \frac{C_o}{C_L}$; $b = \frac{BR^2T^2}{\beta^2}$

Definitions

A = cross-sectional area of diffusion path, cm^2

a,b = constants describing Langmuir isotherm, dimensionless
= constants describing Freundlich isotherm, dimensionless
= derived parameters used with the Dubinin-Radushkevich equation, dimensionless

B = factor used in the Dubinin-Radushkevich equation to describe pore size distribution, $moles^2/calorie^2$

C = equilibrium concentration of adsorbate over adsorbent, g/cm^3

C_o = ambient concentration of adsorbate, g/cm^3

C_L = vapor density of the adsorbate in equilibrium with pure liquid adsorbate at the ambient temperature, g/cm^3

c = ratio of C to C_o, dimensionless

D = diffusion coefficient for adsorbate in air, cm^2/s

k = linear adsorption coefficient, cm^3/g

L = width of air gap between ambient air and sampling surface, cm

m = mass of adsorbent, g

n = index for infinite series

R = ideal gas constant, calories/mole-°K

r = derived parameter used with the Langmuir isotherm, dimensionless

T = ambient temperature, °K

t = sampling time, s

v_o = factor in the Dubinin-Radushkevich equation giving the pore volume per gram of adsorbent, cm^3/g

W = uptake of adsorbate at an equilibrium vapor concentration of C, g

W_o = value of W at C_o, g

w = ratio of W to W_o, dimensionless

$\dot{w}$ = sampling efficiency, defined as the ratio of the actual sampling rate to the maximum sampling rate, dimensionless

β = factor in the Dubinin-Radushkevich equation describing adsorbate-adsorbent interaction, dimensionless

ρ = density of liquid adsorbate at the ambient temperature, g/cm^3

τ_h = nondimensionalized time

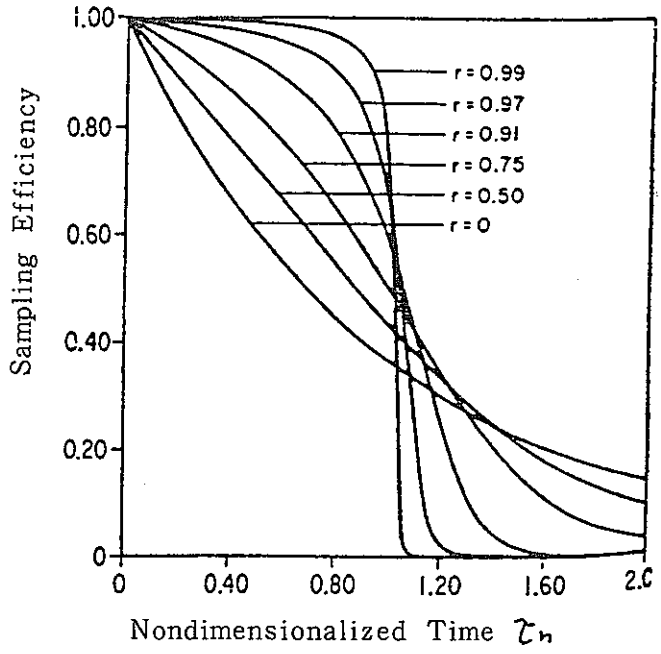

(1) Langmuir Isotherm

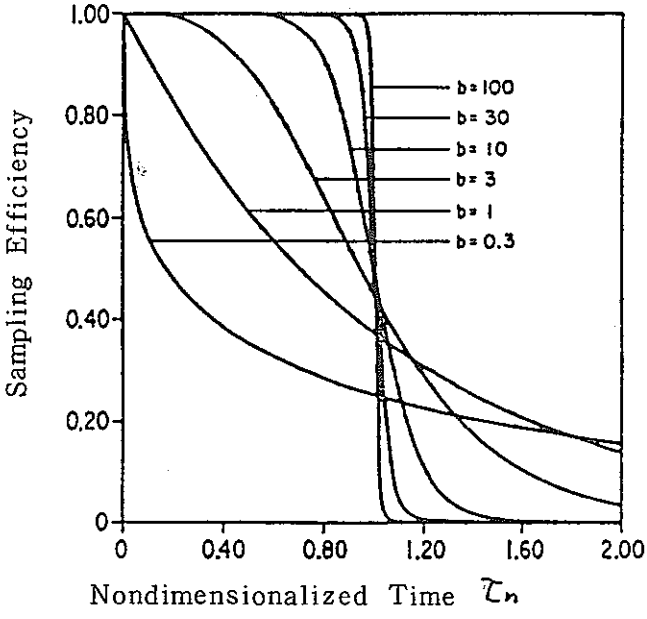

(2) Freundlich Isotherm

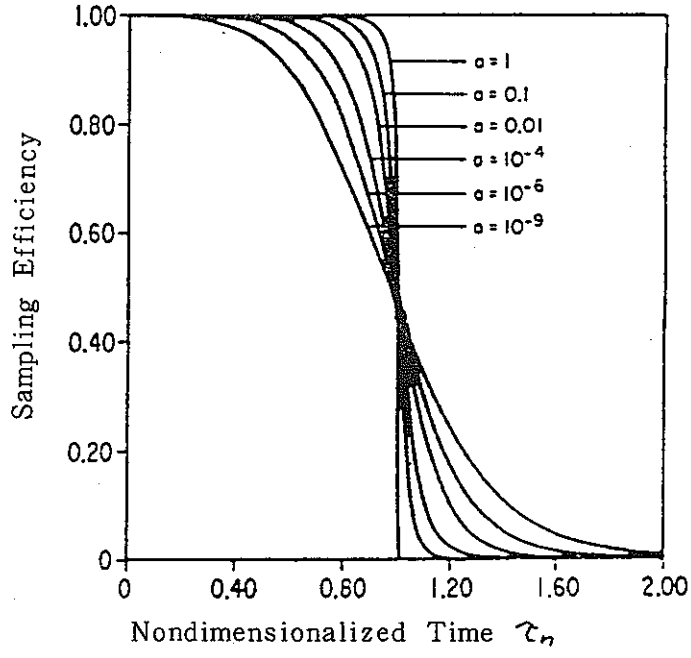

(3) Dubinin-Radushkevich Isotherm

Fig.3-3 Sampling efficiency, as calculated from the nonlinear isotherm (Und84)

3.2.2 Factors Affecting Passive Sampling

(1) Temperature Effects

It is known that the diffusion coefficient is directly proportional to the absolute temperature (T) of the vapor, raised to three-halves power and inversely proportional to the atmospheric pressure (P). However, at the same time, changes in temperature and pressure also affect the ambient concentration of gases. The concentration is inversely proportional to the temperature and directly proportional to the pressure (Tom77, Ros82). That means,

$$D \propto T^{2/3}/P, \qquad C \propto P/T \tag{3-18}$$

As given in equation (3-2), the sampling rate of gases is proportional to the ambient concentration and the diffusion coefficient. Then,

$$dW/dt \propto D\,C \propto T^{1/2} \tag{3-19}$$

Eventually, the sampling rate is only affected by the inverse of square root of temperature (Tom77, Ros82). For practical situations, the temperature effect on the sampling rate seems to be small.

Even if the sampling rate from ambient air to the collection medium surface is not significantly affected by the temperature, the adsorption on the collection medium may be affected by temperature. Underhill and Moeller conducted a literature review of the published experimental data for adsorption of krypton and xenon on activated charcoal (Und80). They used the Antoine equation to summarize data on different temperature conditions. The Antoine equation is expressed as,

$$k = \exp(A + B/(C + T)) \tag{3-20}$$

where,

k	:	Adsorption coefficient (cm^3/g)
A,B,C	:	Antoine coefficients
T	:	Temperature (C)

A,B,C are coefficients depending on adsorbate and carrier gas. Their study gives the typical data on temperature effects of krypton in Fig.3-4.

Strong and Levins give temperature effects of radon adsorption on charcoal for open-end dynamic column as shown in Fig.3-5. They concluded that over the temperature range, 0 - 55 C, the dynamic adsoption coefficient for radon on activated charcoals with specific surface areas (S) in the range 1000-1300 m^3/g can be estimated from the following equation (Str81).

$$k = (0.0070\ S - 3.51)\ \exp(-6.9 \times 10^3/RT) \qquad (3\text{-}21)$$

The temperature effects of xenon, krypton and radon are plotted together in Fig.3-6. Within the temperature range of 0 to 50 C, a relationship similar to equation (3-21) may apply to krypton and xenon.

(2) Water and Organic Vapor Adsorption

When multiple sampling takes place, the compound of gases or vapors with the highest affinity will be adsorbed preferentially for the available adsorption sites on the charcoal surface. The worst interfering substance is believed to be water vapor. Harper suggests that water is adsorbed onto surface oxygen complexes of activated charcoal by hydrogen bonding. Although there are still doubts about the mechanism involved, the further adsorption of water appears to occur by secondary aggregation of these primary sites until the charcoal will block the adsorption of hydrophobic vapors (Har87).

The adsorption of water vapor on various materials is given in Fig.3-7 (McB32). The two central curves on the diagram represent the adsorption of water by different types of charcoal. It is seen that little adsorption capacity has been taken up when the relative pressure = 1/3, and most of it has taken up when the relative pressure = 2/3.

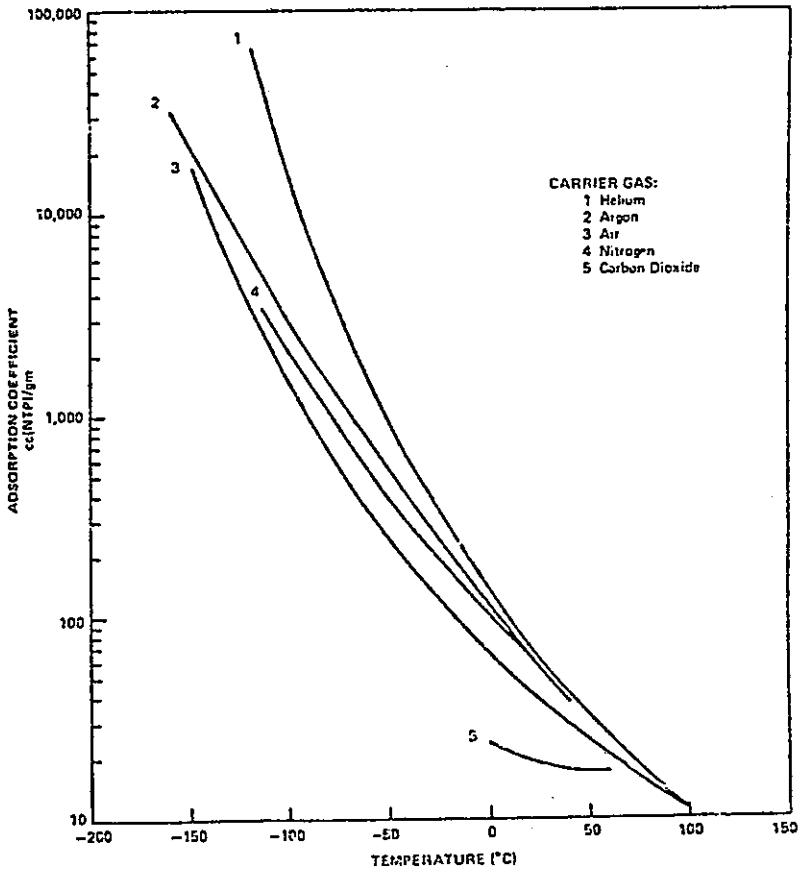

Fig.3-4 Temperature dependence of the adsorption coefficient of krypton (Und80)

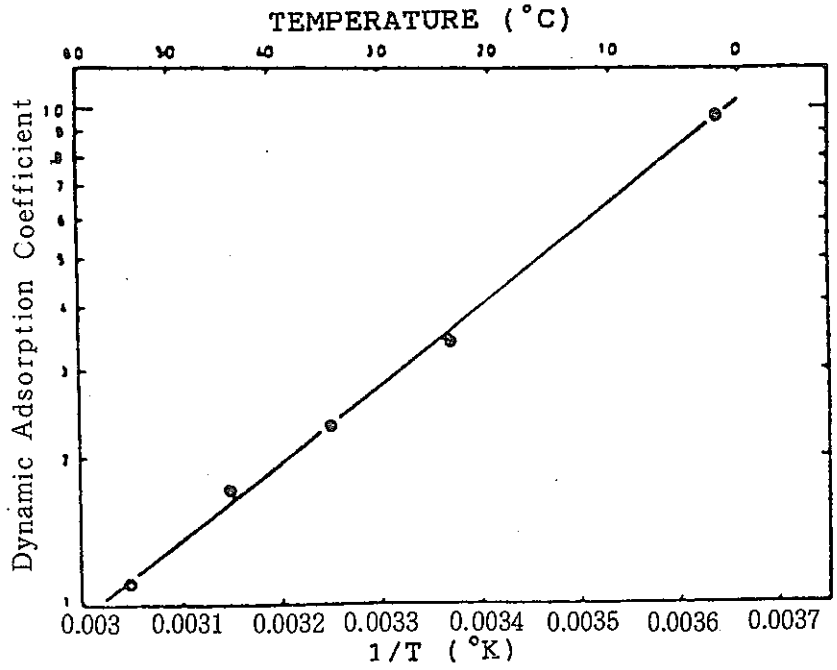

Fig.3-5 Temperature dependence of the dynamic adsorption coefficient (Str81)

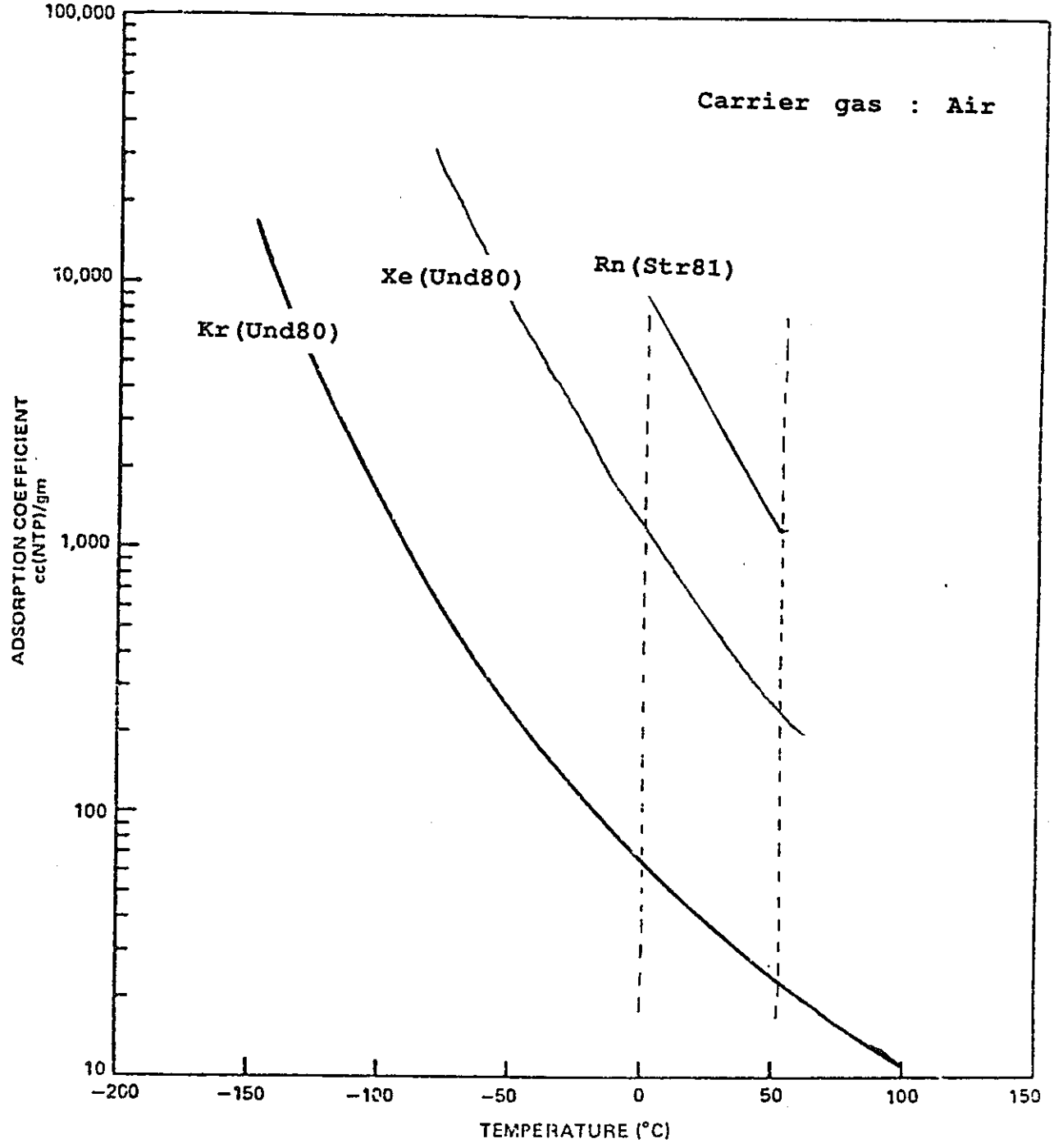

Fig.3-6 Temperature dependence of the adsorption coefficient of krypton, xenon and radon

Fig.3-8 shows an isotherm of carbon disulfide and water vapor obtained by Coolidge on a sample of coconut charcoal (Bru43). It is possible that the structure of charcoal is not entirely rigid, and that both its surface and its pore diameter are functions of the adsorbate molecules. The charcoal can be assumed to consist of a layer-like structure. The force of interaction between the carbon atoms of the adsorbent and the carbon disulfide molecules may be sufficiently strong to permit the latter to penetrate between the layers with comparative ease.

On the other hand, the interaction between charcoal and water is weak, which makes it difficult for water to penetrate between carbon layers. At low pressures there is very little penetration, but some water molecules succeed in penetrating. With increasing pressure it becomes easier for other molecules to penetrate, owing to the large dipole attraction between the water molecules themselves. Eventually, a sharp rise in adsorption occurs, until the capacity is filled. The second explanation is based on the assumption that both isotherm represent unimolecular adsorption. The carbon disulfide curve is a Langmuir isotherm as given in Fig.3-8.

Grant et al. determined the adsorptive capacities of activated carbon pre-equilibrated with moisture for ternary organic gases with paraffins, aromatics and halocarbons, and compared it with similar results for dry gas and dry activated carbon. The use of the Dubinin-Polanyi potential theory and a model which postulates that adsorbed water reduces the pore space available for adsorption on one to one volume basis proved adequate to predict the effect of moisture on the breakthrough capacity of a mixture containing low concentrations of dichloroethylene, n-hexane and toluene. The best agreement was observed in the case of a non-uniform adsorbate model. However, the model did not predict the breakthrough capacity of the relatively soluble methylene chloride in a ternary mixture which included n-heptane and

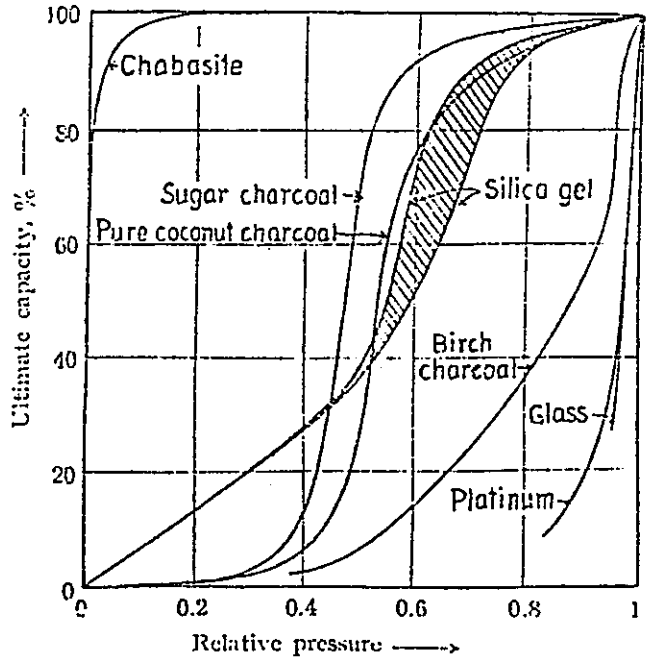

Fig.3-7 Adsorption of water vapor by various materials (McB32)

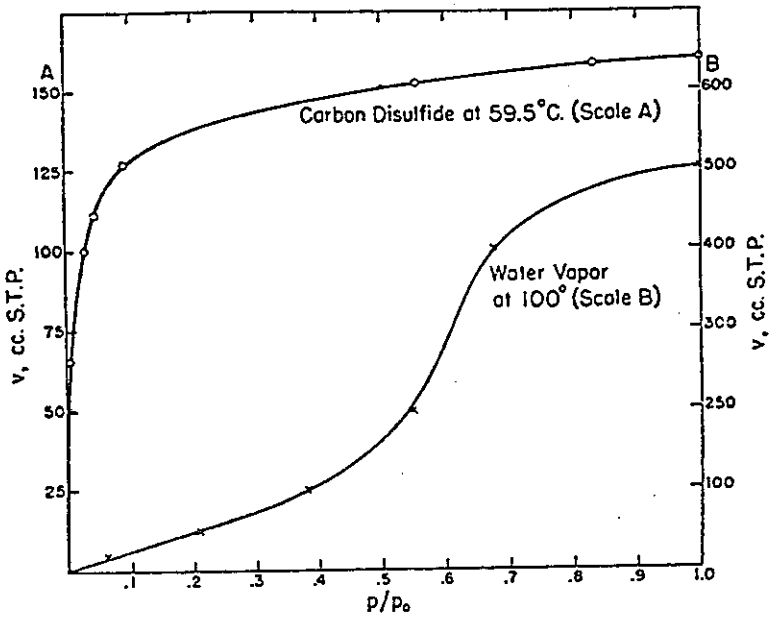

Fig.3-8 Adsorption isotherm of carbon disulfide and water on charcoal (Bru43)

toluene. They concluded that the model used in their report need further study for water insoluble adsorbates (Gra84).

Werner experimentally demonstrated a reduction in uptake of trichloroethylene (TCE) at five relative humidity ranges. Fig.3-9 gives the relationship of adsorbed TCE and relative humidity. The effect of humidity was greatest at the lowest TCE influent concentration (300 mg/m^3) and highest relative humidity involved (86%). Under these conditions the amount of TCE adsorbed was only 9 % of the amount adsorbed at the same concentrations and lowest relative humidity (5%). The effect of humidity was negligible at the highest TCE concentrations (1000 and 1300 mg/m^3) and moderate level of relative humidity (25%). His experimental data fit the Dubinin-Polanyi equation as given in Fig.3-10. (Wer85).

(3) Effect of Moisture on Adsorption of Gaseous Radionuclide

Nuclear power reactors use activated charcoal beds to remove and hold up noble gases to reduce atmospheric radioactive discharge. Underhill and Moeller reviewed published data to quantify adsorption of krypton and xenon on activated charcoal (Und80). The experimental data were usually reported either in terms of the relative humidity of the carrier gas or in terms of the water content of the charcoal. Using a least square analysis, Castellani et al. found that the percent loss in the adsorption coefficient for krypton, from the value at zero percent relative humidity (RH), could be expressed by the following equation (Und80).

$$\Delta k = (0.0037 + 0.0007)\ RH \qquad (3\text{-}22)$$

The effect of the relative humidity of the carrier gas and the water content of an activated charcoal has been examined by Khan et al. According to the examination of their data, Underhill et al. concluded that the effect of water on the adsorption of radioactive fission gases are better correlated with the water content of the charcoal than with the ambient

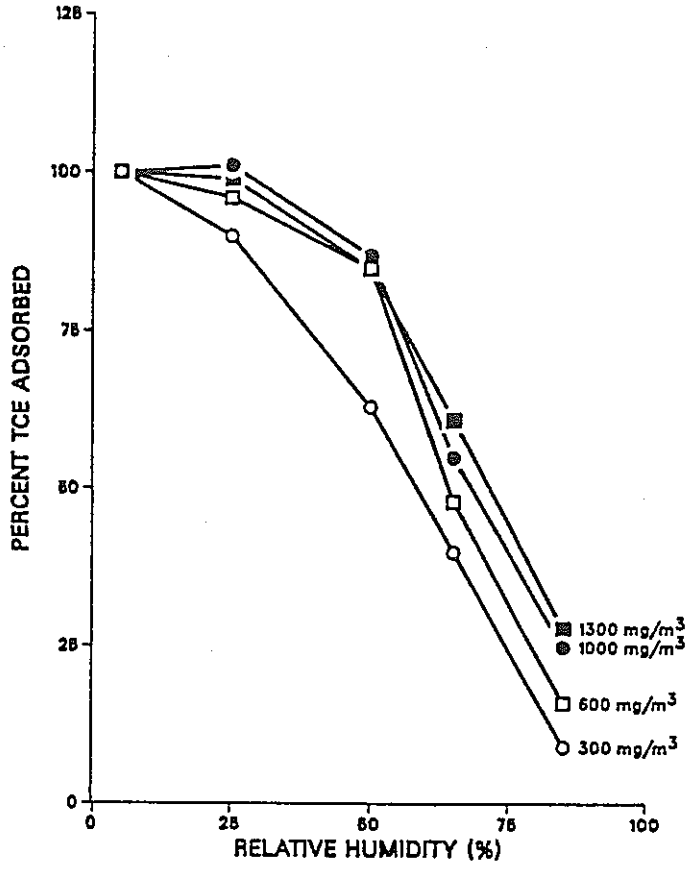

Fig.3-9 Percent of Trichloroethylene (TCE) adsorbed at each level of humidity (Wer84)

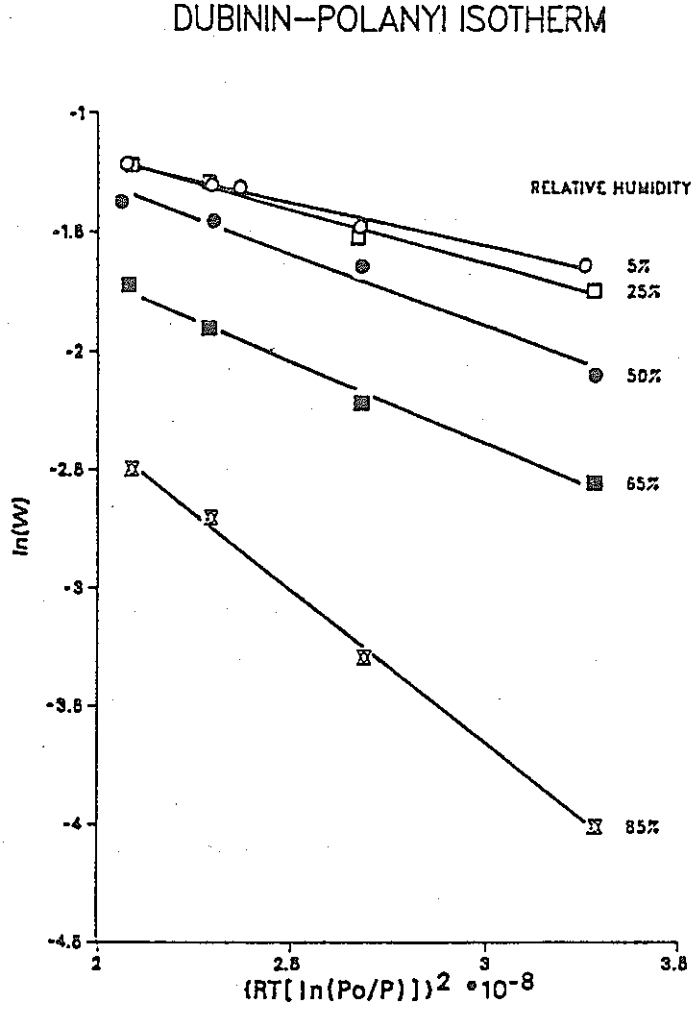

Fig.3-10 Experimental results fit to the Dubinin-Polanyi isotherm (Wer84)

relative humidity of the carrier gas (Und80). Underhill et al. demonstrated the moisture effect on the adsorption of xenon, experimentally. The results of experiment is given in Table 3-2 (Und86). The charcoals are pre-equilibriated with humidified air before the exposure of xenon. At low relative humidity, the uptake of water is small and therefore the reduction in the adsorption of xenon is also small. Fig.3-11 gives the correlation between water uptake and the percent reduction in the adsorption coefficient. The adsorbed amount of xenon decrease as the moisture content increase. Fig.3-11 is plotted in Fig.3-12 as a semi log graph in terms of the moisture uptake and the percent reduction of adsorption coefficient. The adsorption coefficient seems to decrease exponentially as the moisture uptake increases.

The effect of moisture on the radon adsorption was experimentally demonstrated by Strong and Levins (Str81). A radon pulse was introduced into a charcoal column with humidified air. Fig.3-13 shows that the dynamic adsorption coefficient decreased by 30 percent for an increase in relative humidity from 0 to 100 percent. This effect is explained by the observation that the radon penetrates the bed at a faster rate than water vapor. Hence, for most of this travel, the radon passes through the dry charcoal bed. Near the inlet, the combined effects of temperature rise due to the heat of adsorption of water and the competition with water vapor for active sites tends to reduce the dynamic adsorption coefficient for radon.

The above results (Und86, Str81) are plotted in Fig.3-14 in terms of relative humidity and percent reduction of adsorption coefficient. The reduction of adsorption coefficient is different in the two experiments due to experimental conditions. In the experiment by Strong and Levins, the humidified air was passed into the dry bed with a radon pulse. Hence, the charcoal was not pre-equilibriated with water. In the experiment by Underhill et al., the charcoal was pre-equilibriated at appropriate humidity

Table 3-2 Effect of Moisture on the Adsorption of Xenon (Und86)

Relative Humidity(%)	Uptake of Water (wt %)	Reduction in Adsorption Coefficient (%)
7.7	0.5	5
14	1.0	8
27	1.6	19
44	5.7	38
59	23	83
67	31	94

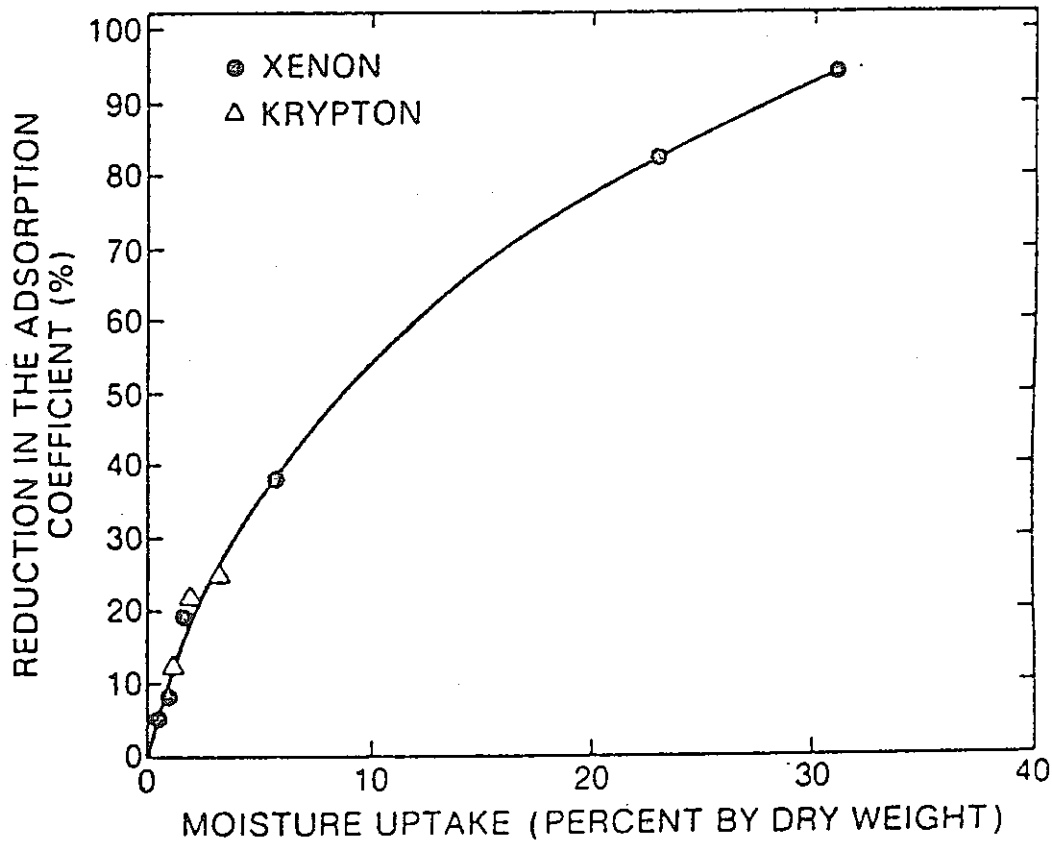

Fig.3-11 Effect of moisture on the adsorption of krypton and xenon (Und86)

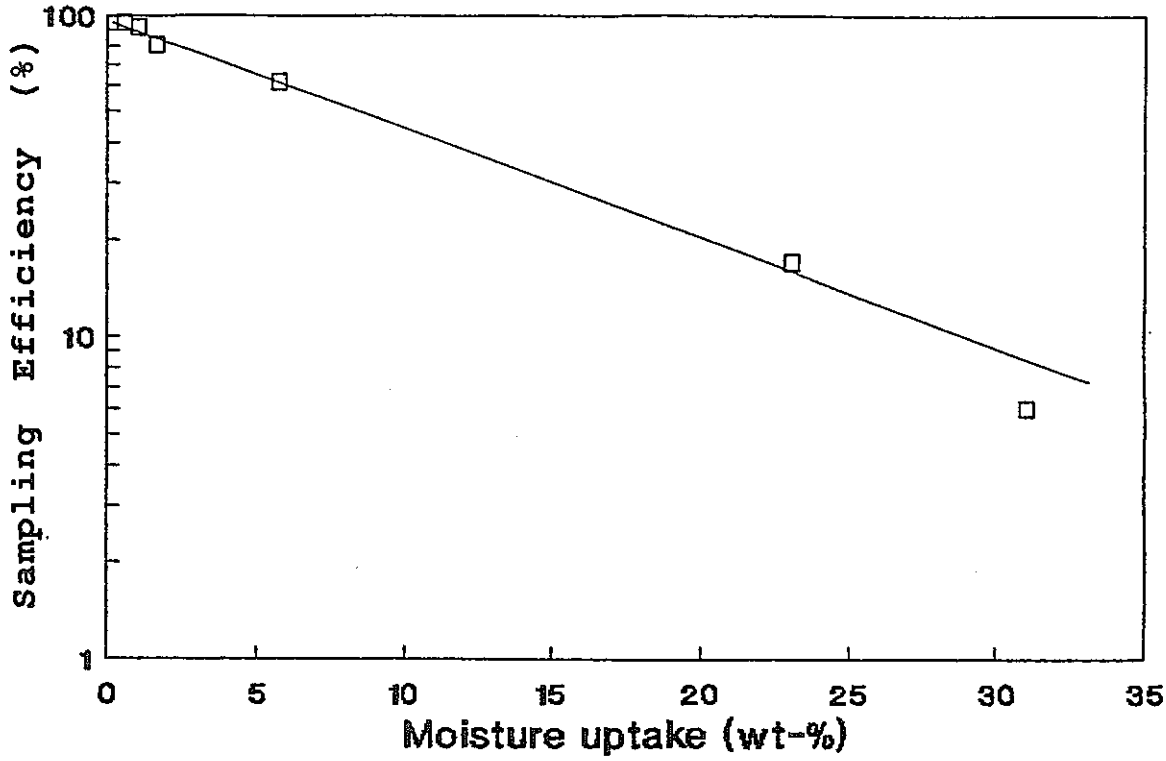

Fig.3-12 Effect of moisture on the adsorption efficiency of xenon

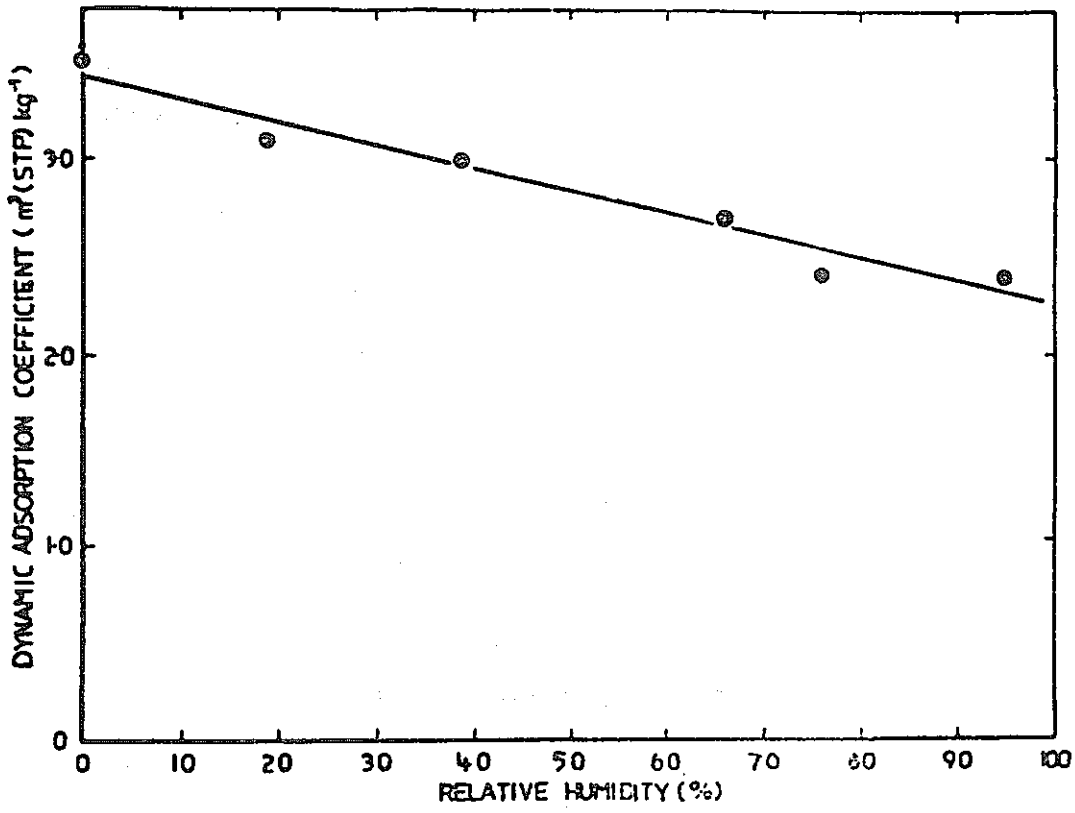

Fig.3-13 Effect of relative humidity on the dynamic adsorption coefficient of radon (Str81)

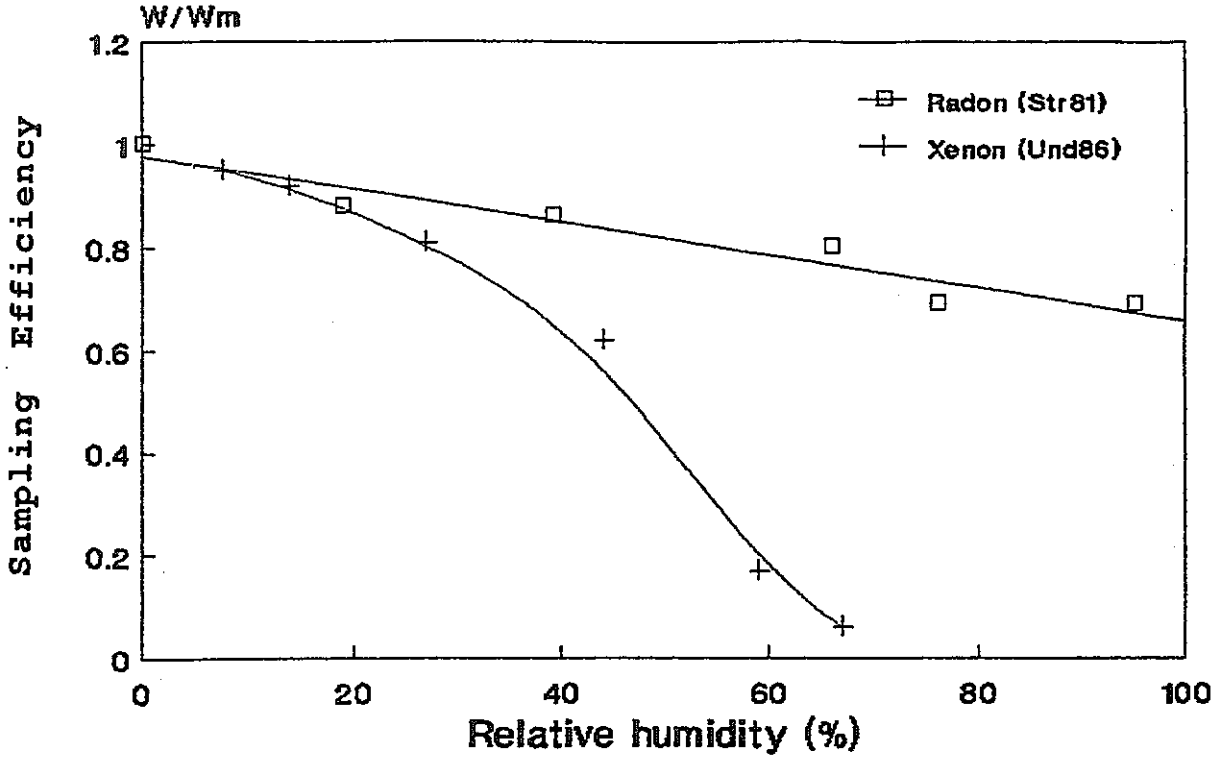

Fig.3-14 Effect of relative humidity on the adsorption efficiency of xenon and radon

conditions before exposure to xenon. In passive sampling, simultaneous adsorption of moisture and gases takes place. Initially, the relationship of moisture and adsorption coefficient may be represented by results of Strong and Levins. The extended sampling period allows equilibrium of moisture, and the ultimate situation may be represented by the results of Underhill et al.

(4) Surface Area of Charcoal

Kovach and Etheridge observed that the adsorption coefficient for krypton was a maximum if the charcoal was activated to give a surface area of 900 square meters per gram (Fig.3-15). The data developed by these authors show that the adsorption coefficients for krypton and xenon are not proportional to the surface area of the adsorbent, and that high surface area and/or pore volume are not necessarily indicators of higher adsorption capacity for krypton and xenon (Und80). In the experiment with radon by Strong and Levins, the linear relationship between surface area and the adsorption coefficient was observed (Fig.3-16, Str81). Underhill noted that causes for this difference in the relationship has not been observed for krypton and xenon compared to radon are not known (Und80).

Table 3-2 Effect of Moisture on the Adsorption of Xenon (Und86)

Relative Humidity(%)	Uptake of Water (wt %)	Reduction in Adsorption Coefficient (%)
7.7	0.5	5
14	1.0	8
27	1.6	19
44	5.7	38
59	23	83
67	31	94

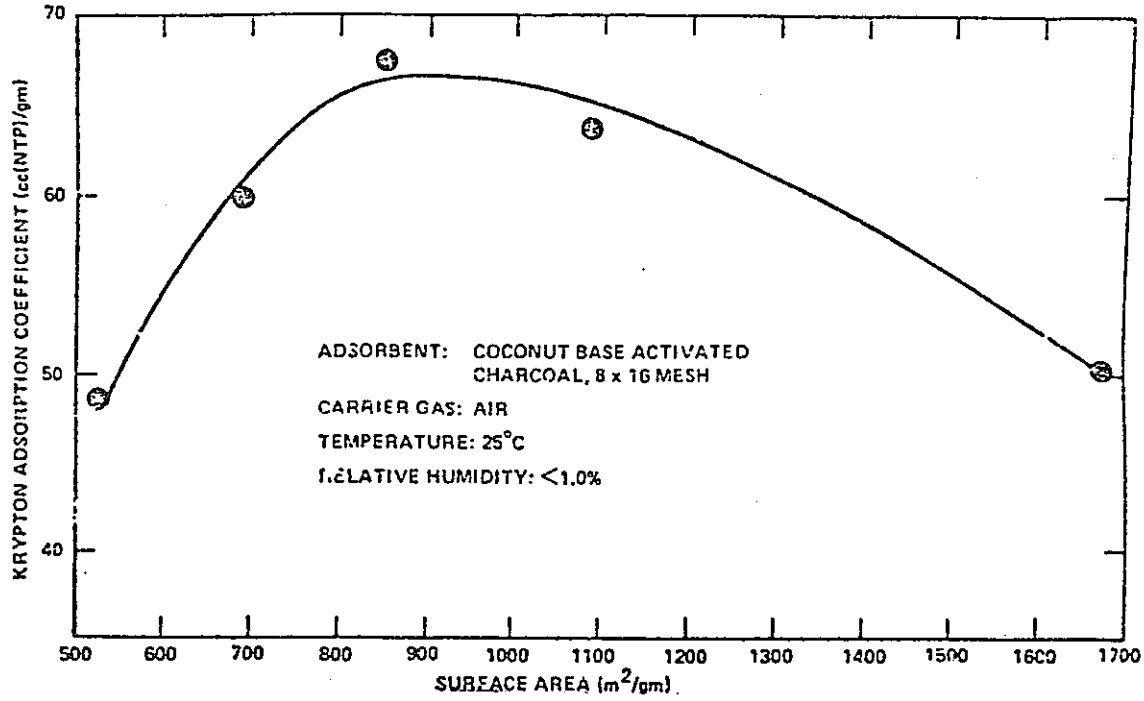

Fig.3-15 Relation between surface area of charcoal and adsorption coefficient of krypton (Und80)

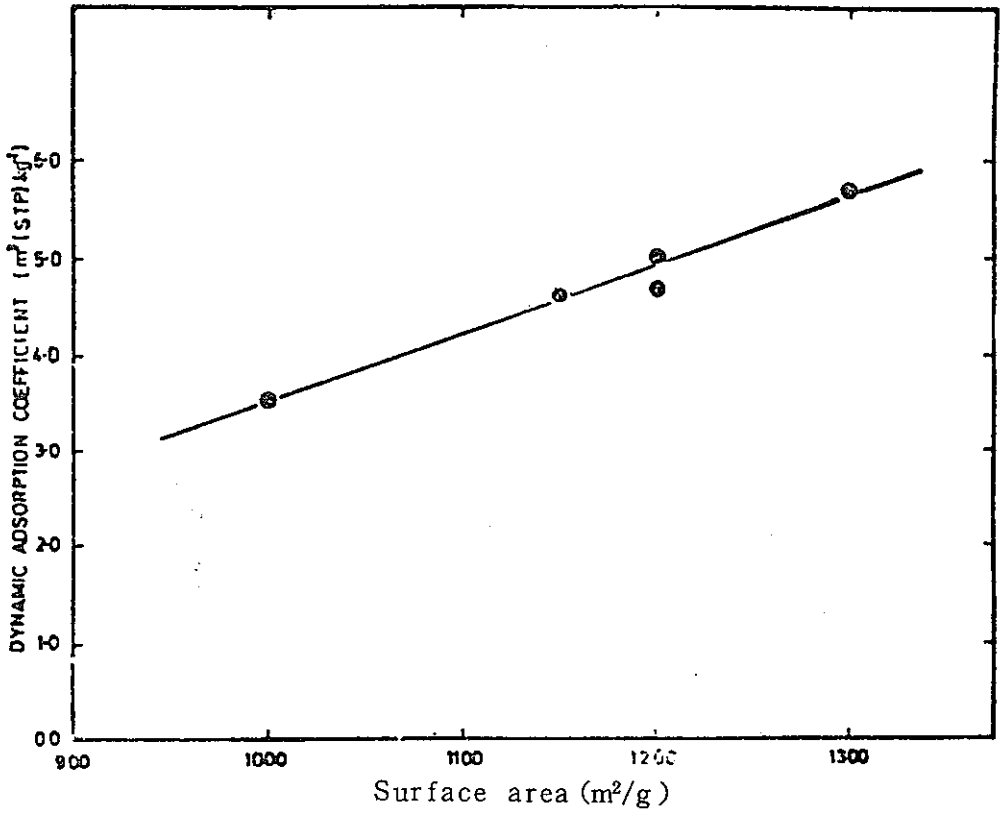

Fig.3-16 Relation of surface area of charcoal and adsorption coefficient of radon (Str81)

(5) Determination of Adsorption Coefficient

Previously obtained data for open-end dynamic samplers were given for krypton, xenon and radon (Und80, Str81, Und84, Und86). The closed-end passive charcoal samplers were developed by Cohen, George and Prichard for the monitoring of indoor radon concentration (Coh83, Coh86a, Geo84, Pri85). It is useful to compare the methods for determining the adsorption coefficient for dynamic and passive sampling in this section.

Concerning the adsorption of organic vapor, Van den Hoed et al. made field comparisons of a diffusive sampler (3M monitor) and charcoal tube sampler for styrene (Van87). The field tests show good agreement between the average results as obtained by the two techniques. Besides radiological decay, the behavior of a radionuclide and other adsorbates may be basically the same.

The major difference between dynamic and passive sampling is in the determination of the adsorption coefficient. In passive sampling, the adsorption coefficient is simply expressed by the ratio of the adsorbed amount of adsorbate on the charcoal to the ambient concentration.

$$k = \frac{\text{Adsorbed amount of adsorbate on the charcoal (Bq/g)}}{\text{Ambient air concentration (Bq/cm}^3\text{)}} \qquad (3\text{-}23)$$

In dynamic sampling, the gaseous radionuclide is introduced to the charcoal column as a pulsed input, and the exhaust flow is measured by a detection device such as an ionization chamber. The dynamic adsorption coefficient is determined by integration of the exhaust concentration over the total volume. The typical method to calculate dynamic adsorption coefficient is given by Underhill (Und86).

$$k = \frac{\int_0^\infty VC_x\,dV}{m\int_0^\infty C_x\,dV} - \frac{Vd}{m} \qquad (3\text{-}24)$$

where,

V : Volume of effluent following the pulse injection (cm^3)

Vd : Volume of ionization chamber plus volume of tubing between the adsorbent bed and the ionization chamber (cm^3)

Cx : Radioactivity in the effluent, as measured by the ionization chamber (Bq/cm^3)

Because the measurement is by ionization chamber, the concentration in the exhaust flow over the total volume is integrated. Sun and Underhill showed that the above equation, which states implicitly that the measured adsorption coefficient is independent of the concentration of adsorbate and the geometry of the adsorption bed, is valid at the low concentrations of xenon and krypton normally found in reactor off-gas streams.

The adsorption coefficient is basically given by the ratio of the radionuclide captured in charcoal to the ambient concentration. Typical values of adsorption coefficient given in the literatures are summarized in Table 3-3. Because the adsorption coefficient is given for various type of charcoals and experimental conditions, the adsorption coefficients vary. Radon is most strongly adsorbed on the charcoal among the three nuclides.

Table 3-3 Typical data on the adsorption coefficient

Radionuclide	Adsorption coefficient (cm^3/g)
Krypton	20 - 60 (Und77, Und80)
Xenon	100 - 900 (Und77, Und80)
Radon	2000 - 6000 (Str81, Coh83)

(6) Face Velocity

The velocity of the air external to the charcoal may have significant effect. On the diffusion coefficient and possibly the adsorption coefficient, the velocity of the air external to the charcoal is often referred to as face velocity. Thompkins and Goldsmith noted that the passive sampler can be expected to sample accurately as long as essentially all resistance to contaminant transport is contained within the stagnant air layer inside the device. As the face velocity decreases, the external resistance to mass transfer associated with convection increases. When this resistance becomes significant, the mass of contaminant collected will become less than predicted (Tom77).

As Jonas et al. subsequently noted, the face velocity directly affects the concentration gradient. In the case of a minimum face velocity parallel to the open face of the sampler, starvation of the external atmosphere may result (Jon81). The prominence of this effect will be related to the sampling rate (DA/L) which is a function of geometry (A/L). Badge-type samplers have a high area to length ratio and therefore high uptake rate, which requires a minimum face velocity of 0.05 - 0.1 m/sec. These samplers therefore should not be employed for static monitoring in areas of little air movement (Har87).

Samplers are also affected by high face velocity causing turbulence to occur within the diffusion air gap. Wind tunnel experiments have shown that, provided the length to diameter ratio (L/d) is greater than 2.5-3.0, this will not affect performance significantly (Har87).

(7) Diffusion Coefficient

A method for estimating diffusion coefficients is given by Underhill (Und77). The formula is expressed as,

$$D = \gamma \varepsilon' Dg/\rho c\ k \qquad (3\text{-}25)$$

where

Dg : Diffusion coefficient for the gas in the air (cm^2/s)

γ : Tortuosity factor for the charcoal

ε' : Fractional interparticle void volume

ρ_c : Density of the charcoal (g/cm^3)

k : Adsorption coefficient (cm^3/g)

Dg depends on atomic size, mass, and thermodynamic properties of nuclide. Underhill determined Dg for krypton and xenon as 0.173 cm^2/s and 0.138 cm^2/s, respectively. He also noted typical values of the tortuosity factor = 0.6 and the fractional interparticle void volume = 0.45, and determined D for krypton and xenon as 1.6×10^{-3} cm^2/s and 7.0×10^{-5} cm^2/s, respectively (Und77). Cohen subsequently derived Dg = 0.12 cm^2/s and D = 1.6×10^{-5} cm^2/s for radon based on Underhill estimates (Coh83).

The typical values of the diffusion coefficients for krypton, xenon and radon are summarized in Table 3-4 (Und77, Coh83). In terms of the diffusion coefficient, radon is a less diffusive nuclide compared with krypton and xenon. For the diffusion coefficients of organic and other vapors in air, the report by Lugg provides comprehensive information (Lug68).

Table 3-4 Typical data on the diffusion coefficient

Radionuclide	Diffusion coefficient (cm^2/s) in the air	in the charcoal
Krypton	0.173(Und77)	1.6×10^{-3}(Und77)
Xenon	0.138(Und77)	7.0×10^{-5}(Und77)
Radon	0.12(Coh83)	1.6×10^{-5}(Coh83)

(8) Time Averaging

Cohen et al. validated the effectiveness of the diffusion barrier charcoal adsorption (DBCA) collector for environmental concentrations of radon through comparison with other methods such as track etch and continuous monitor (Coh86b, Coh88). Through comparison with a continuous monitor, uncertainties involved in time averaging of short-term fluctuations using DBCA collectors for 1 month average indoor radon measurement were estimated to be approximately 12 %. They concluded that in the view of the many other greater sources of uncertainty in deriving the desired information, the 12 % average uncertainty due to lack of time averaging over short-term fluctuations in the DBCA collector is acceptable.

3.3 Moisture Effects on Passive Sampling of Radon

3.3.1 Experiment

To quantify the adsorption mechanism of radon with moisture in the air, a chamber experiment was designed by Kahn and Gray in 1986-1987 (Kah87). The charcoal used in this series of experiment is commonly used for the environmental monitoring by the Environmental Protection Agency (EPA). Schematic diagram of the geometry of the charcoal sampler is given in Fig.3-17. The samplers were exposed in the chamber for radon concentration of 26 mBq/l (0.7 pCi/l) with levels of humidity at the EPA Eastern Environmental Radiation Facility.

Experimental conditions are specified as follows.

Sample

Charcoal Weight	:	70 g/Cartridge
Pretreatment of Charcoal	:	None
Ambient Radon Concentration	:	26 mBq/l (0.7 pCi/l)
Ambient Air temperature	:	Room temperature

Measurement

Counting Device	:	Gamma ray detection
Counting Efficiency	:	7.4×10^{-12} count/min. per Bq (0.275 count/min. per Ci)
Counting time	:	10 min.
Decay Factor	:	0.98

The relative humidity conditions were determined in seven ranges such as 21-27 %, 33-44 %, 50-55 %, 58-62 %, 62-77 %, 78-84 % and 95-98 %. Because of difficulty in keeping these conditions constant, humidity has a wide range. The experiments at three humidity ranges of 21-27 %, 50-55 % and 78-84 % were for the period of 12 days. In this series of experiments, after 6 days of exposure in the radon, air without radon was introduced to the chamber to determine turnover of radon from the EPA charcoal.

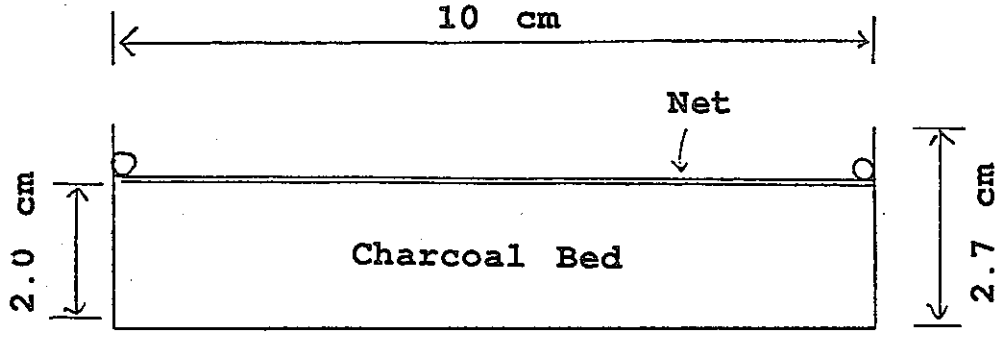

Fig.3-17 Geometry of EPA Charcoal

3.3.2 Results

The experimental data are given in Table 3-5 and 3-6. The adsorbed amount of radon on the EPA charcoal (W) is normalized by charcoal mass (m = 70 g) and ambient air concentration (Co = 26 mBq/l), and given in unit of Bq/g-charcoal per Bq/cm^3-air, or cm^3/g. The normalized adsorption amount (W/mCo) of radon was corrected for radiological decay. Fig.3-18 gives time-dependent ingrowth of W/mCo. Using equation (3-14) with the diffusion coefficient of radon, D = 1.3 x 10^{-5}, the depth of the EPA charcoal of 2 cm gives the estimate of time required to reach equilibrium as,

$$Teq = 3.6 \text{ days} \qquad (3\text{-}26)$$

As shown in Fig.3-18, W/mCo seems to saturate in the lower humidity ranges (< 50 %) within a few days. This is reasonable with the projected equilibrium time. Further reduction of the adsorption coefficient is indicated in the higher humidity ranges (> 50 %). Turnover of radon from the charcoal is given in Fig.3-19. The turnover constant for 21-27 % humidity seems to be 0.58 (1/d). Different values may be given for other relative humidities. According to Fig.3-11 - Fig.3-14, reduction of the adsorbed amount of radon depends on the adsorption of water. To account for later reduction of radon, interference of water with radon adsorption should be considered.

The adsorption of water on the EPA charcoal was measured in the unit of increased weight percent relative to initial weight (wt-%). Time dependent ingrowth of water content (Wc) is given in Fig.3-20. Wc is saturate in the lower humidity ranges (< 50 %) within several days. However, further adsorption of water is measured for higher humidity ranges (> 50 %). This might affect the adsorption of radon on the EPA charcoal. More detailed discussion is given in the following section.

Table 3-5 The adsorption of radon on the EPA charcoal, as represented by W/mCo (Bq/g-charcoal per Bq/cm^3-air)

Time	Relative Humidity in the Ambient Air (%)						
(Day)	21-27	33-44	50-55	58-62	62-77	78-84	95-98
1	2,600	2,500	2,600	2,400	2,500	2,300	2,100
2	3,700	3,500	3,200	3,100	2,800	2,600	2,400
3	4,400	3,800	3,300	3,300	2,600	2,200	1,900
4	4,600	4,000	3,300	3,200	2,300	1,900	1,300
5	4,800	-	3,300	-	-	1,500	-
6	4,800	-	3,200	-	-	1,200	-
7	(2,500)	-	(1,300)	-	-	(190)	-
8	(1,500)	-	(630)	-	-	(11)	-
9	(840)	-	(270)	-	-	(-)	-
10	(470)	-	(120)	-	-	(-)	-
11	(300)	-	(64)	-	-	(-)	-
12	(150)	-	(34)	-	-	(-)	-

a. Figures in parenthesis are data in the absence of radon.

Table 3-6 Adsorption of water on the EPA charcoal (Increased weight percent by initial weight)

Time	Relative Humidity in the Ambient Air (%)						
(Day)	21-27	33-44	50-55	58-62	62-77	78-84	95-98
1	-0.9	-0.2	1.7	2.3	5.0	6.0	8.0
2	-1.0	0.2	2.6	4.0	9.2	11	14
3	-1.1	0.5	3.9	5.6	12	15	20
4	-1.1	0.6	4.4	6.7	15	19	25
5	-1.1	-	5.0	-	-	22	-
6	-1.3	-	5.7	-	-	25	-
7	-1.1	-	5.4	-	-	26	-
8	-1.3	-	5.4	-	-	29	-
9	-1.0	-	5.6	-	-	31	-
10	-1.0	-	5.6	-	-	33	-
11	-0.9	-	5.8	-	-	36	-
12	-1.0	-	6.4	-	-	36	-

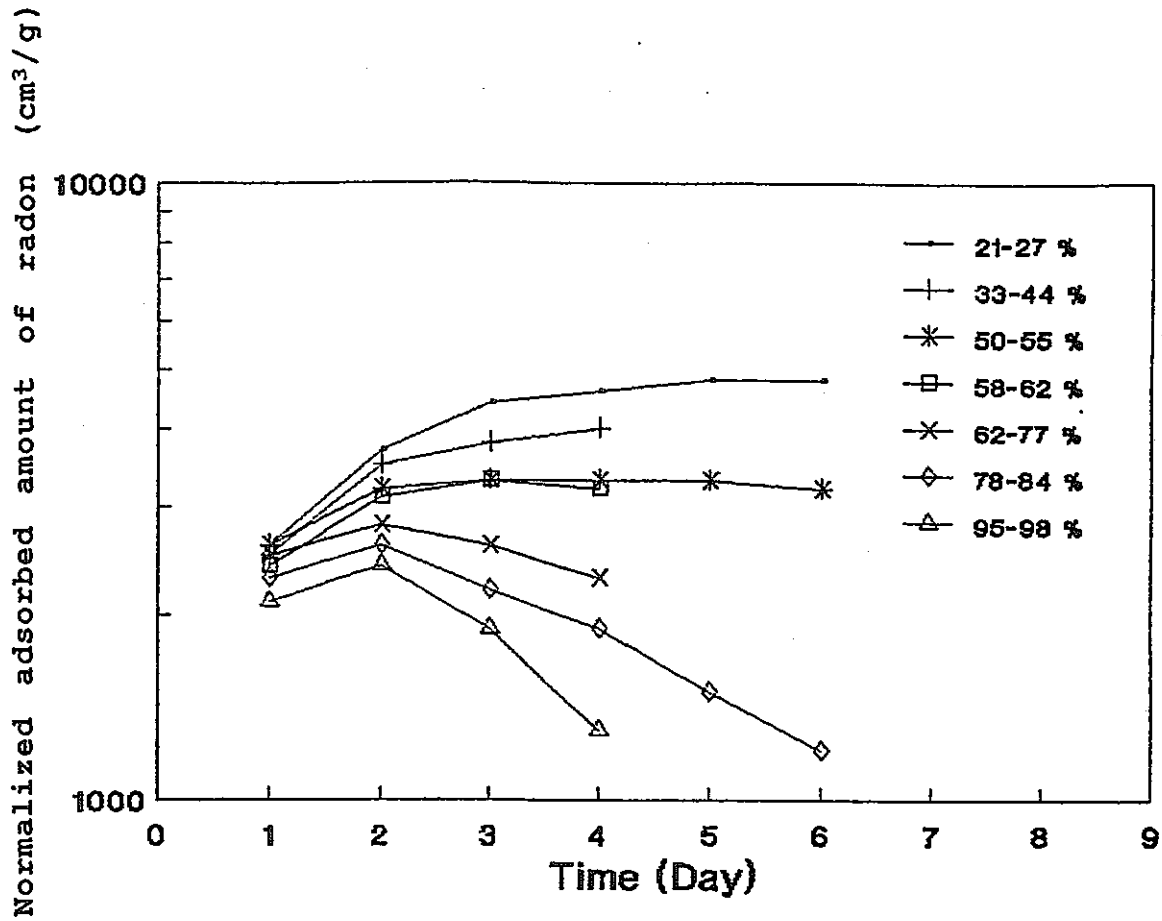

Fig.3-18 Adsorption amount of radon on the EPA charcoal represented by W/mCo

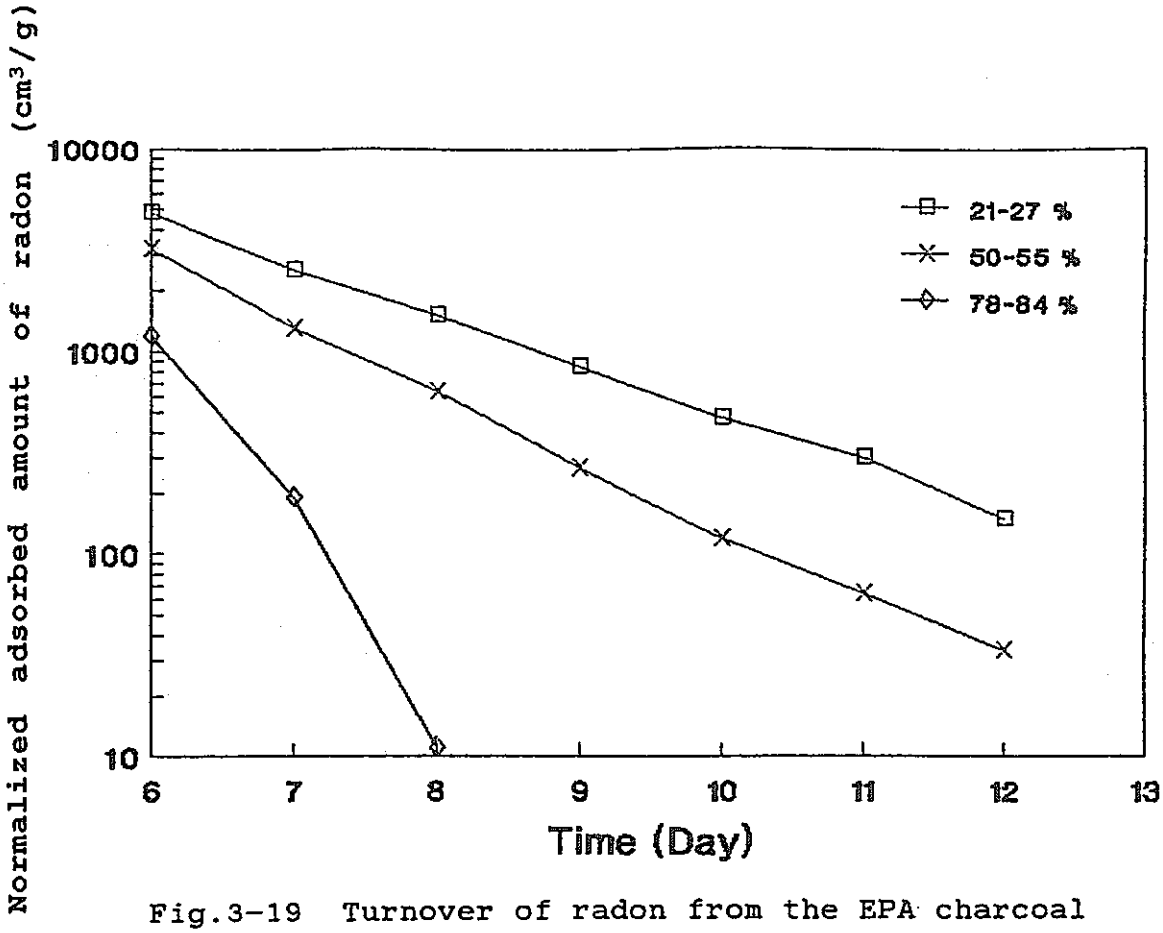

Fig.3-19 Turnover of radon from the EPA charcoal

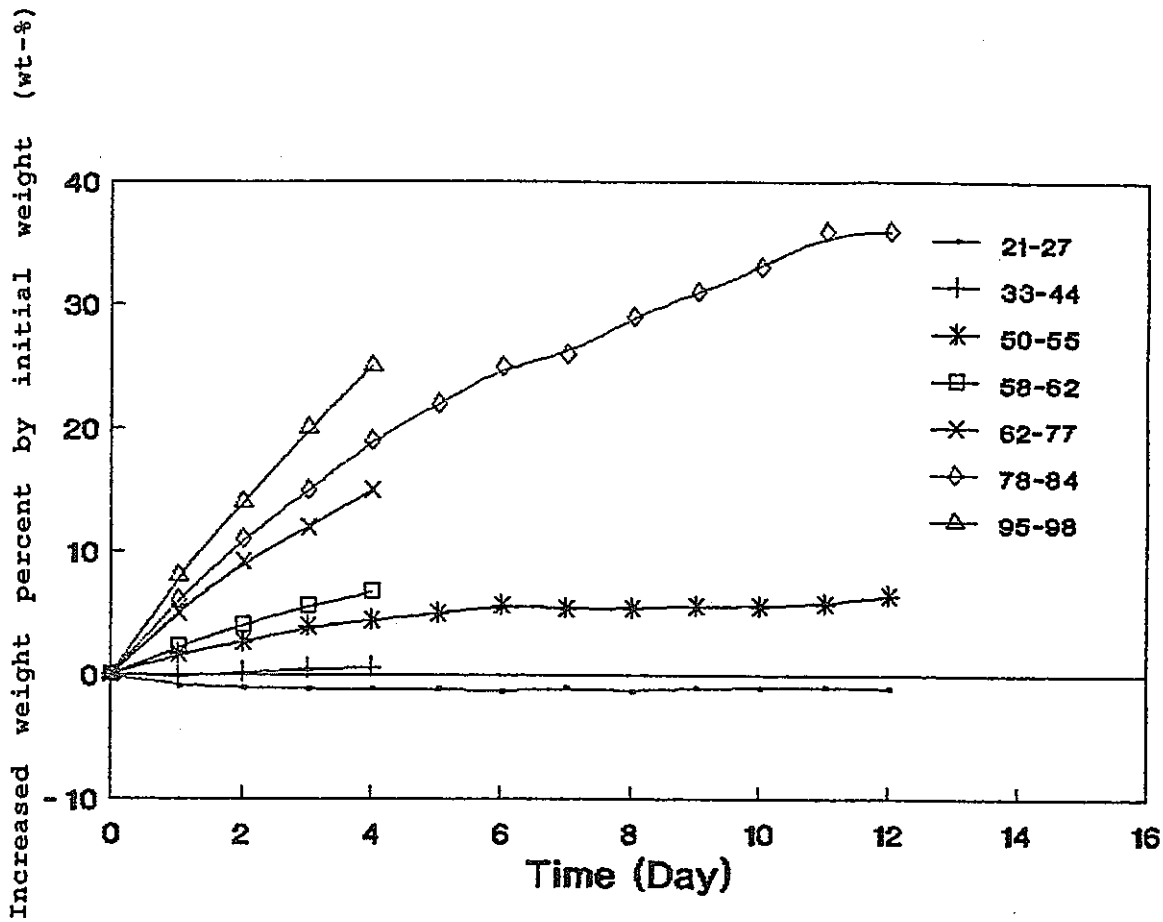

Fig.3-20 Adsorption of water on the EPA charcoal represented by increased weight percent

3.3.3 Discussion

(1) Adsorption of Water

As given in 3.2.1 (2), previously demonstrated data for water and organic vapor show good agreement with potential theory (Reu77, Chi77, Fre77, Wer84). It seems useful to start from the Dubinin-Polanyi equation to describe adsorption of water on charcoal. Equations (3-15) and (3-17) give adsorbed volume of water per gram charcoal (cm^3/g-charcoal) as follows.

$$Wv = Wm \exp(- kc \varepsilon^2) = Wm \exp(- kcR^2T^2\ln^2(P/Po)) \quad (3\text{-}27)$$

By definition, the relative humidity (RH) is the ratio of the partial pressure to the saturated partial pressure. P/Po can be expressed by relative humidity.

$$Wv = Wm \exp(- kcR^2T^2\ln^2(RH/100)) \quad (3\text{-}28)$$

Because the measured data of adsorbed amount of water on the charcoal is given in the increased weight percent relative to initial weight, it is useful to express equation (3-28) in the same quantity. The increased water content (Wc) is given by,

$$Wc = 100\ Wv = 100\ Wm\ \rho \exp(- kcR^2T^2\ln^2(RH/100)) \quad (3\text{-}29)$$

where, 100 is the conversion factor to express unit in percent, and ρ is the density of water (1.0 cm^3/g). R is the gas constant (1.987 cal/mol/ K), and T can be assumed to be room temperature (298 K) in this experiment. RH is determined by experimental conditions. Wm and kc are the charcoal specific values.

Werner demonstrated the effectiveness of the Dubinin-Polanyi isotherm as given in Fig.3-10. Fig.3-21 gives the Dubinin-Polanyi isotherm plot for ln(Wc) and ε^2. The data for exposure times of 2nd day, 4th day and 12th day are plotted. Experimental data fit the Dubinin-Polanyi isotherm. As shown in equation (3-16), kc can be given as slope of the line, and

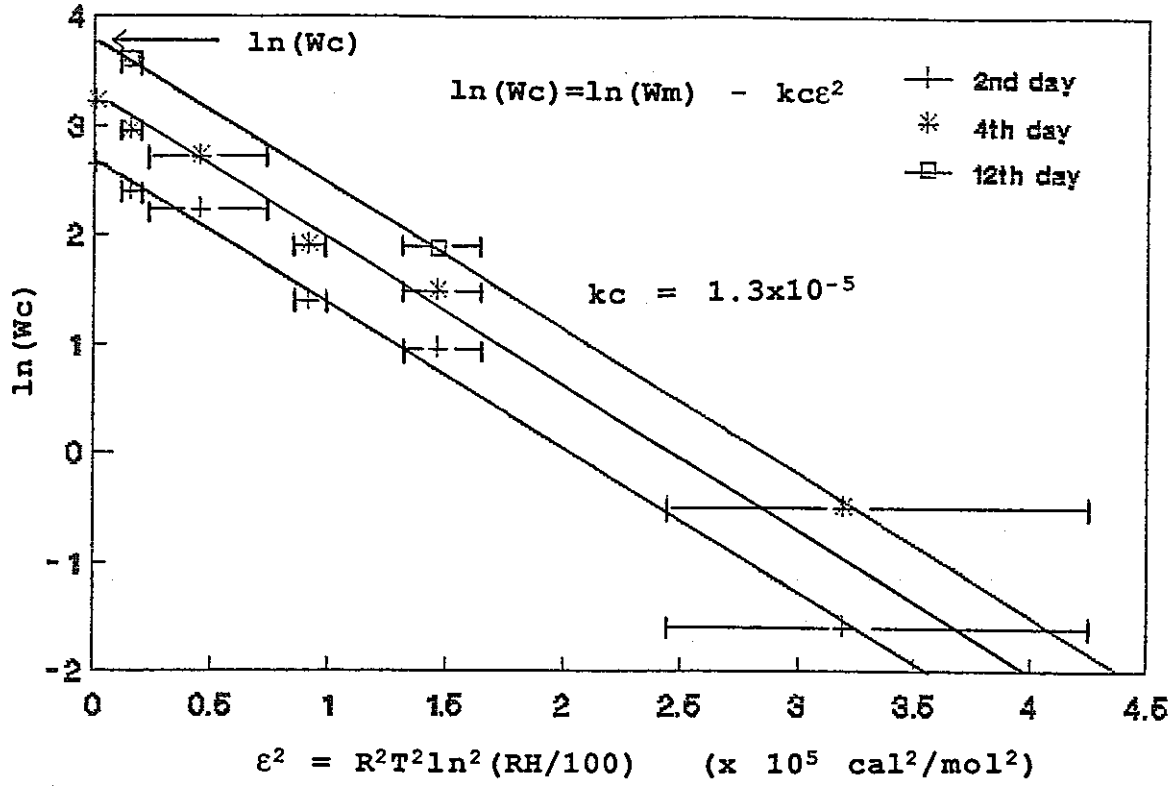

Fig.3-21 Experimental data fit to the Dubinin-Polanyi isotherm

Wm as saturated value at $\varepsilon^2 = 0$. According to Fig.3-21, Wm and kc can be assumed to be 1.3 x 10^{-5} (mol^2/cal^2) and 0.46 (cm^3/g), respectively. The equation (3-29) can be written as,

$$Wc=46\exp(-4.6\ \ln^2(RH/100)) \qquad (3\text{-}30)$$

The equilibrium adsorption capacity of water can be calculated by equation (3-30). Calculated values are given in Table 3-7 and plotted in Fig.3-22. The shape of the isotherm curve is similar to those given in Fig.3-7 and Fig.3-8.

The next problem is the time dependence of water content in the pre-equilibrium state. According to Fig.3-22, the water content can be assumed to be proportional to the relative humidity in the relative humidity range of 50 - 80 %, which usually represent the indoor condition.

$$Wc \propto RH \qquad (3\text{-}31)$$

Then, a linear relationship between Wc and RH can be assumed. Fig.3-23 gives the time dependence of differential increase of water content. Although there are significant variations, the turnover constant can be assumed to be 0.2 (1/d, half time = 3.5 d). Using the value of 0.2 (1/d), the time dependence of water content can be expressed by,

$$Wc = 46\ \exp(-4.6\ \ln^2(RH/100))(1 - \exp(-0.2t)) \qquad (3\text{-}32)$$

This equation explains time dependence of increased weight percent by dry weight of the EPA charcoal.

Because the measurement of adsorbed amounts of water is given in units of increased weight percent relative to initial weight, a correction should be made to account for the initially adsorbed amount of water before the exposure in the radon chamber. As given in Fig.3-22, adsorption capacity of water below 30 % humidity is assumed to be zero. Hence, the minimum weight percent given in Table 3-6 can be assumed to be the dry weight of charcoal. Using -1.3 % as the dry weight of the EPA charcoal, equation (3-32) can be re-written as follows.

Table 3-7 Equilibrium adsorption capacity of water on EPA charcoal, as calculated by equation (3-30)

Relative Humidity	Increased weight percent (%)
>30	>0.058
40	0.97
50	5.0
60	14
70	26
80	37
90	44
100	46

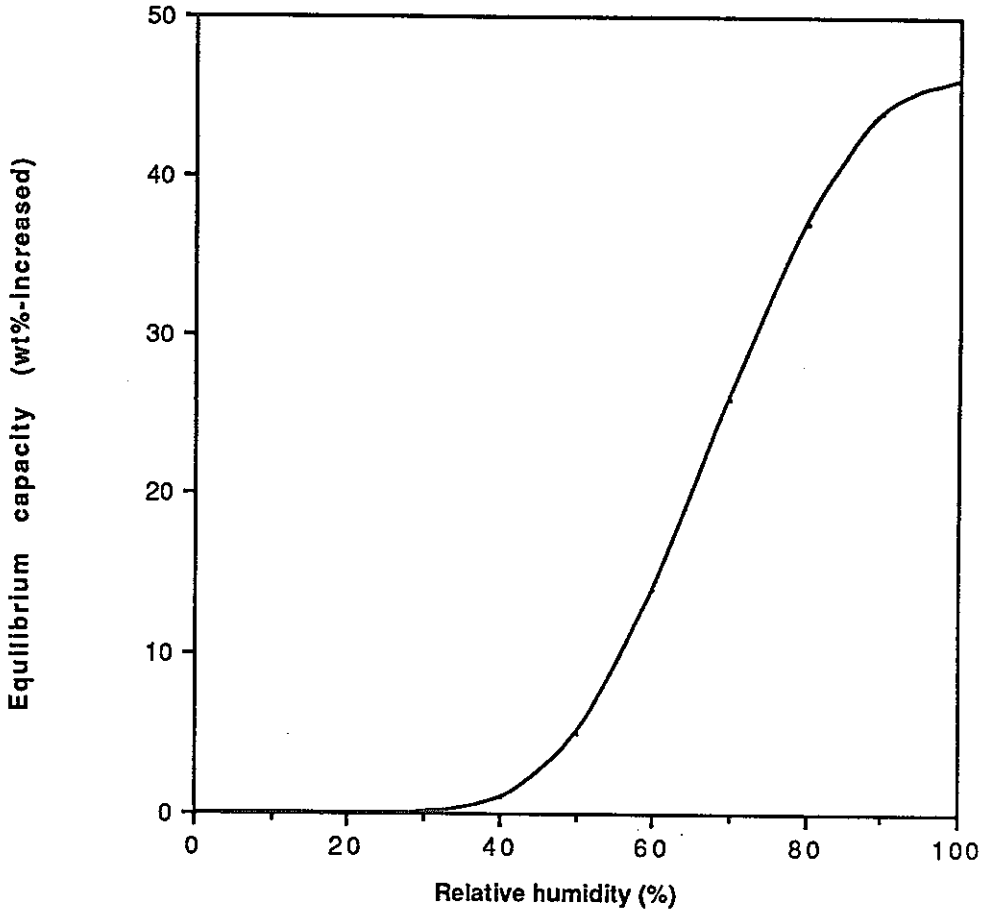

Fig,3-21 Maximum capacity of water adsorption on charcoal

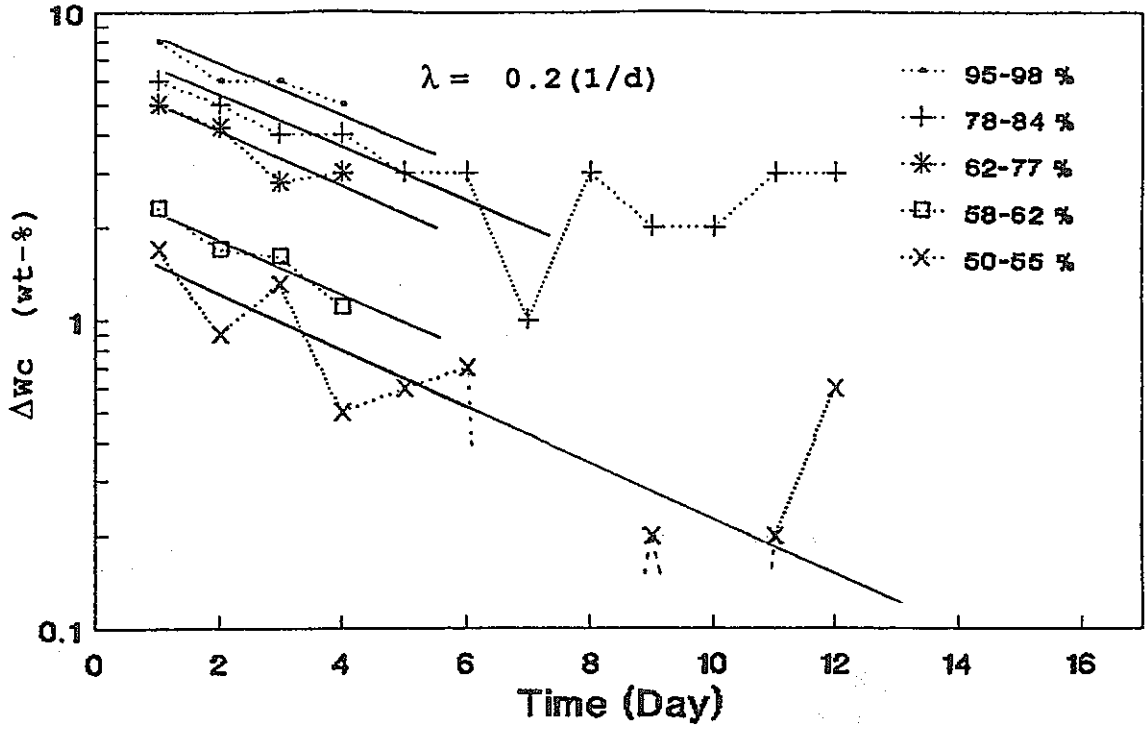

Fig.3-23 Time dependence of differential increase of water content

$$Wc = (47.3\exp(-4.6\ \ln^2(RH/100))-1.3)(1-\exp(-0.2t)) \quad (3\text{-}33)$$

Equation (3-37) is plotted in Fig.3-24 for typical humidity ranges together with measured data. Equation (3-33) seems to represent the adsorbed amount of water given in increased weight percent relative to initial weight.

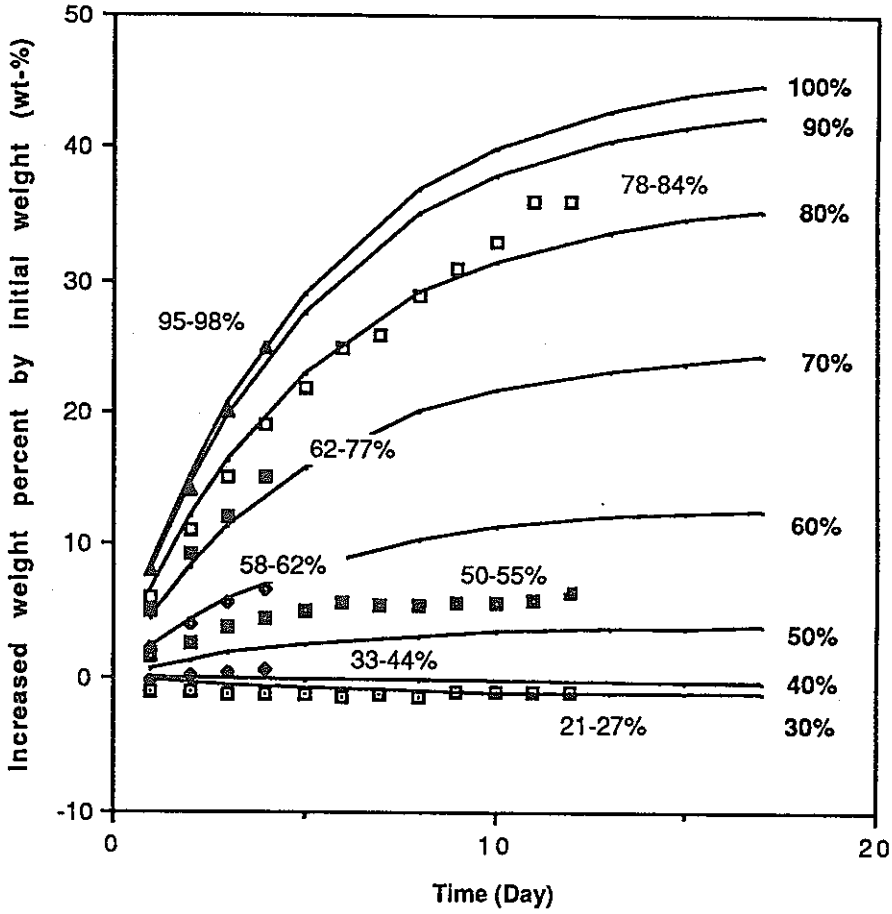

Fig.3-24 Time dependent water content, as calculated from equation (3-33)

(2) Adsorption of Radon

The adsorption coefficient may be correlated with relative humidity or water content. Fig.3-25 gives the normalized adsorption amount of radon (W/mCo) in terms of relative humidity(RH). Experimental data represent the linear relationship between W/mCo and RH as presumed by Strong and Levins (see Fig.3-13).

However, one-to-one correlations with relative humidity are not sound theoretically because of hysteresis in the adsorption and desorption of water. It is more preferable to correlate the reduction of the adsorption coefficient with water content of the charcoal (Und86). Furthermore, for practical application, it is not expected to measure average relative humidity in homes. The water content of charcoal can be easily determined by weighing. Correlation with adsorption and water content should be considered.

As the sampling time becomes large, the normalized adsorption amount of radon (W/mCo) can be assumed to be the adsorption coefficient (k) according to equation (3-6). Fig.3-26 gives effect of water content on W/mCo of radon. Considering the equilibrium, data of time after 3 days are plotted. Fig.3-26 gives the relationship of the adsorption coefficient of radon and water content as,

$$k = 4500 \exp(- 0.049\ Wc) \qquad (3\text{-}34)$$

where, Wc is the water content of the charcoal expressed in the unit of increased weight percent relative to initial weight (%-wt).

As given in Fig.3-22, water adsorption is nearly zero below 30 % relative humidity. Then, the normalized adsorbed amount of radon (W/mCo) of 4,800 (cm^3/g) in Table 3-5 can be assumed to be the maximum adsorption coefficient. Furthermore, -1.3 % of increased weight percent can be the dry weight of the charcoal. Using the maximum k of 4,800 and the dry weight of - 1.3 %, equation (3-34) is plotted in Fig.3-27 in terms of reduction of the adsorption coefficient of radon, together

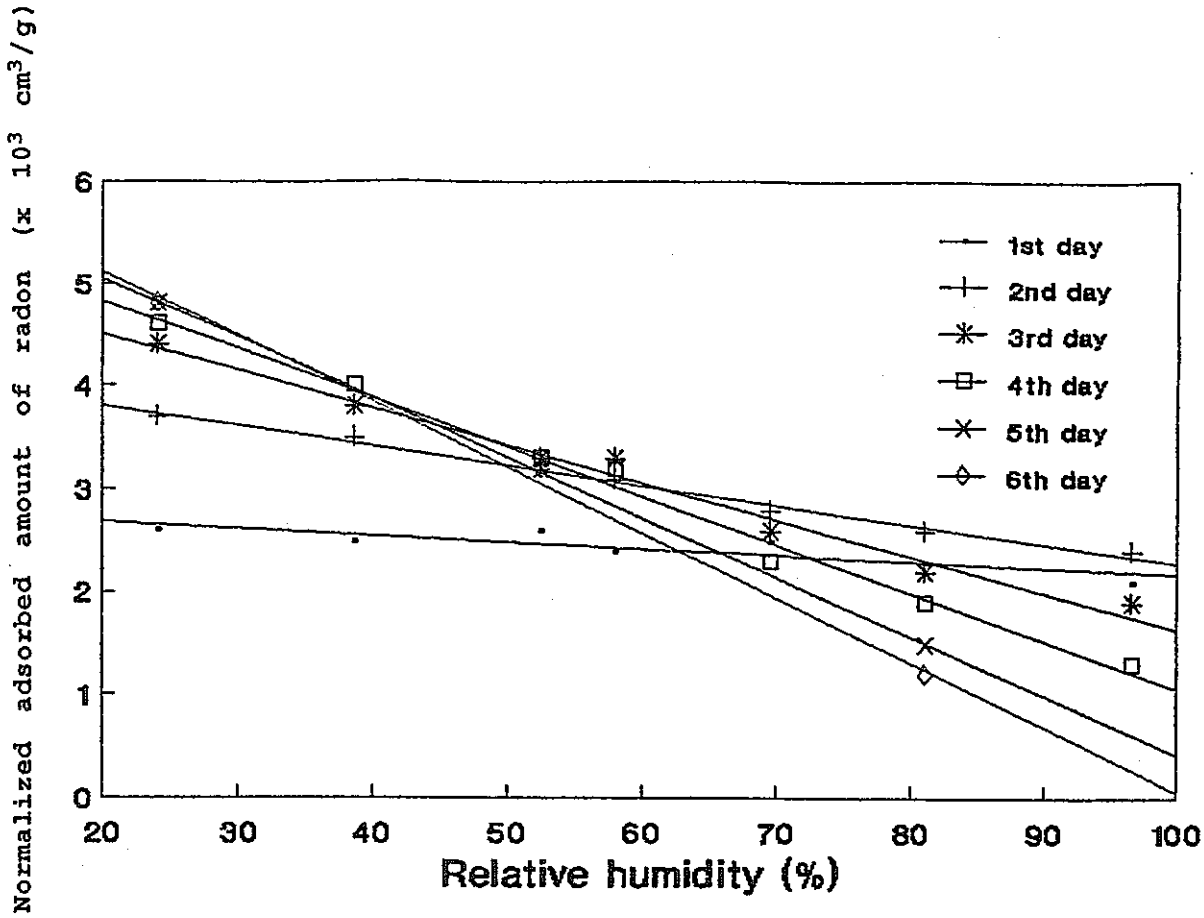

Fig.3-25 Effect of relative humidity on the adsorption of radon

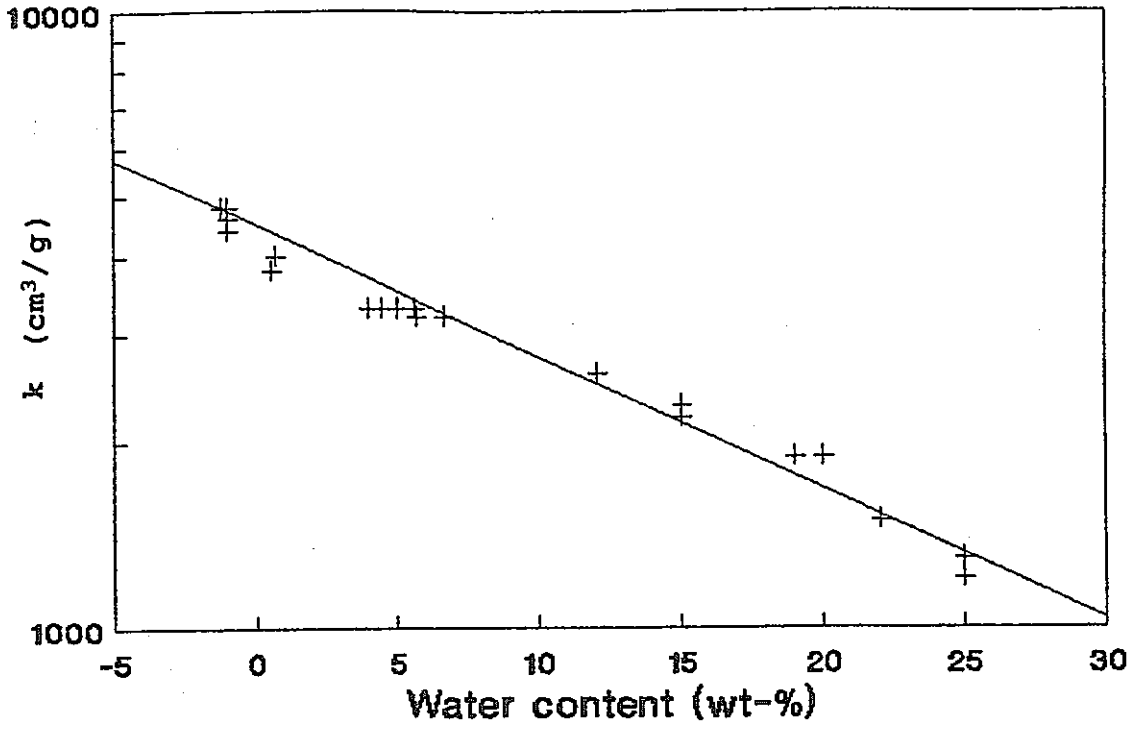

Fig.3-26 Effect of water content on the adsorption of radon

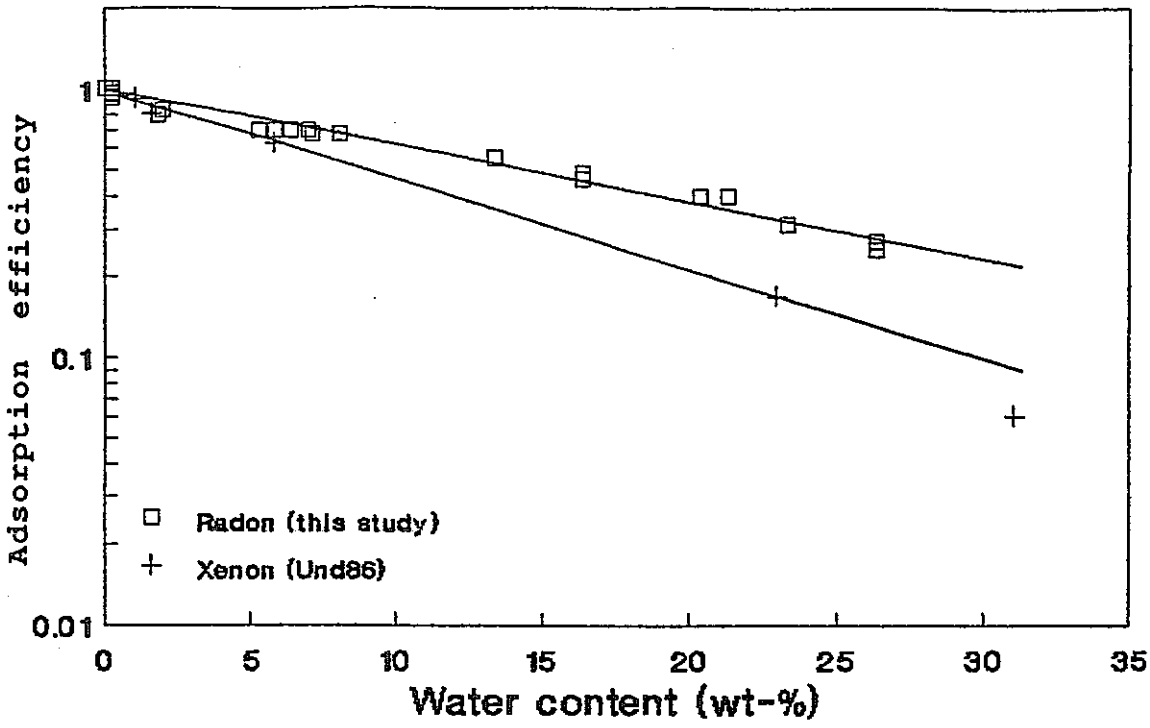

Fig.3-27 Effect of water content on the adsorption of xenon and radon

with that of xenon given by Underhill et al. (Und86). As noted in 3.3.1 (3), the difference of the curve can be characterized by the fact that Underhill's curve is given for charcoal equilibriated with moisture, and the radon curve is given for the experiment of simultaneous adsorption.

The next problem is the time dependent increase of the radon adsorption coefficient. The linear adsorption theory can be assumed for gaseous materials. The time constant can be derived by a turnover experiment. As the ambient concentration of radon, Co, is 0 after the exposure period, equation (3-2) can be written as,

$$dW/dt = - ADC/L \qquad (3\text{-}35)$$

Assuming a linear isotherm, equation (3-35) can be integrated in the same way with equation (3-6).

$$W = Wi \exp(-ADt/kmL) \qquad (3\text{-}36)$$

where Wi is the initial amount of radon just after exposure. This equation explains the turnover of radon from charcoal. As given in 3.3.2 and Fig.3-19, the turnover constant can be assumed to be 0.58 (1/day). The maximum adsorption coefficient for 21-27 % of 4,800 gives,

$$AD/mL = 0.58 \times 4{,}800 = 2{,}800 \ (cm^3/day\ g) \qquad (3\text{-}37)$$

Then, equation (3-40) can be written as,

$$W = Wi \exp(-2{,}800\ t/k) \qquad (3\text{-}38)$$

Using equation (3-34) for determination of k, the turnover of radon from charcoal is plotted in Fig.3-28. Equation (3-38) with equation (3-34) shows good agreement with measured data.

Eventually, equation (3-6) and (3-38) give the normalized adsorbed amount of radon (W/mCo) as,

$$W/mCo = k\ (1-\exp(-2{,}800\ t/k)) \qquad (3\text{-}39)$$

Using equation (3-34) for the determination of k and the measured water content (Wc) in Table 3-6, equation (3-39) is

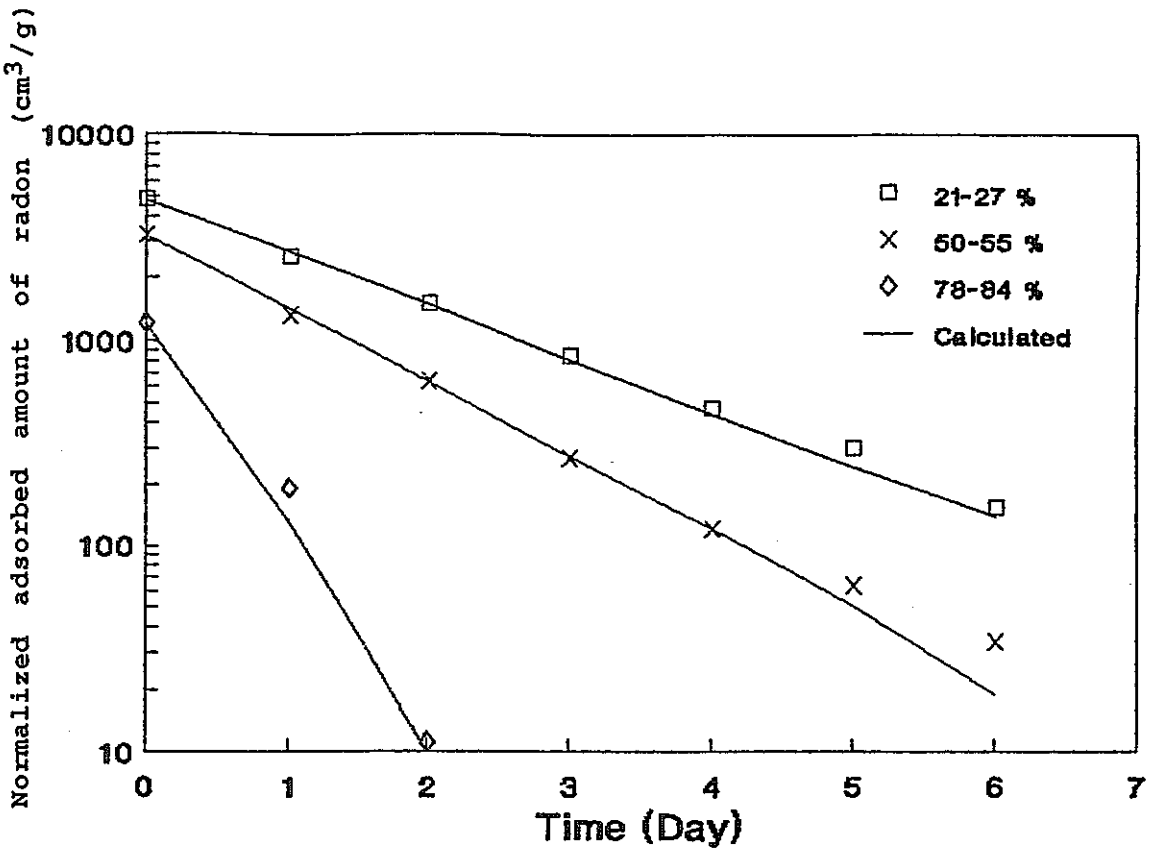

Fig.3-28 Turnover of radon from EPA charcoal, as calculated from equation (3-38)

plotted in Fig.3-29. Because the equilibrium data were taken into account to derive equation (3-34), the pre-equilibrium state is not necessarily consistent with measured data. However, it seems consistent with data in extended sampling period.

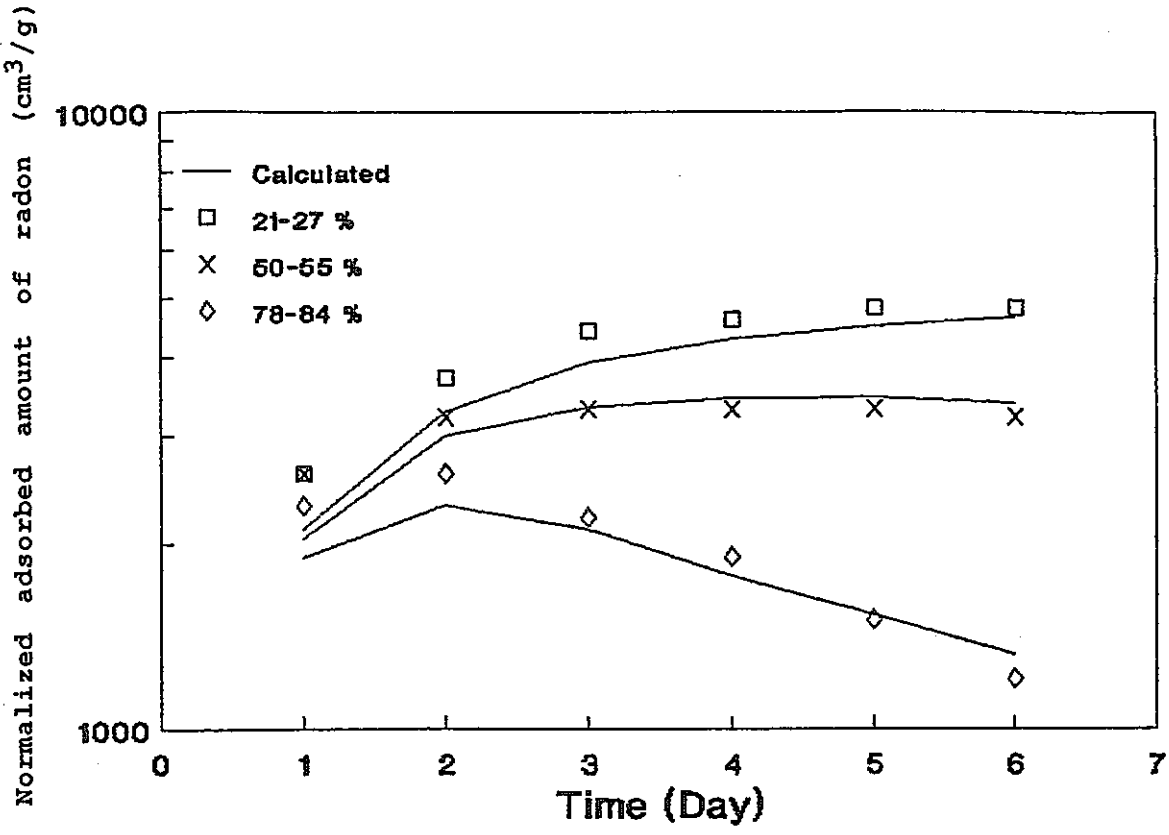

Fig.3-29 Time dependent adsorption of radon, as calculated from equation (3-39) and (3-34)

5. CONCLUSIONS

This study was compiled during Mr.Asano's tenure in Georgia Institute of Technology as a visiting scholar in May 1988 - April 1989. Following three series of equations were presented in this study to describe adsorption mechanism on charcoal.

* Adsorbed amount of water (wt-%)
  $Wc = (47.3\exp(-4.6\ln^2(RH/100))-1.3)(1-\exp(-0.2t))$

* Adsorption coefficient of radon (cm^3/g)
  $k = 4500 \exp(- 0.049\ Wc)$

* Normalized adsorbed amount of radon (cm^3/g)
  $W/mCo = k\ (1 - \exp(-2{,}800\ t/k))$

Using the above equations, the adsorbed amount of radon is calculated as functions of relative humidity and time.

In practical situations, the ambient concentration of radon, Co, is the problem of concern. In the case of the EPA charcoal, m = 70 g. Wc and W can be determined by measurement. If the sampling time t is long enough (more than 3.6 days), the charcoal adsorption can be assumed to reach equilibrium. Then, the ambient concentration of radon is given by following equation.

$$Co = W/(70k(1 - \exp(-2{,}800\ t/k)))$$

Because few data were available to derive above equations, several factors are assumed tentatively in this report. Following further studies are suggested to describe more detail adsorption mechanism of radon on charcoal.

(1) Dry weight of charcoal

Because the dry weight of EPA charcoal was not known, -1.3 % of initial weight was assumed to be the dry weight. Dry weight of charcoal should be used to correct Table 3-6 and derivation of equation (3-33).

(2) Adsorption coefficient of radon in dry weight

Because experimental data are not given for the dry weight of charcoal, maximum value of the normalized adsorbed amount of radon, 4,800 cm^3/g, was assumed to be maximum adsorption coefficient to compare the results of xenon. Adsorption coefficient of radon in dry weight should be measured to correct Fig.3-27.

(3) Computer program to solve nonlinear isotherm

In this report, a linear relationship for relative humidity and water adsorption was assumed to determine time dependent water adsorption. From the practical standpoint, this may be acceptable. However, development of a computer program to calculate the non-linear isotherm will provide a more detail analysis of water adsorption mechanism.

(4) Long-term experiment

In this study, derivation of a set of equations for water adsorption is based on the experimental data up to 12 days. Depending on the required monitoring period, more long-term experiment is necessary to determine well equilibriated situations.

(5) Validation study for adequacy of time averaging

According to the studies by Cohen, uncertainties involved in the time averaging of short-term fluctuations using DBCA collector was estimated to be 12 % (Coh88). A validation study should be designed for the EPA charcoal to quantify uncertainties involved in the charcoal.

REFERENCES :

Alt81 Alter,H.W. and Fleisher,R.L. "Passive Integrity Radon Monitor for Environmental Monitoring", Health Physics Vol.40, pp.696-702, 1981

Bro83 Brown,L. "National Radiation Survey in the U.K. : Indoor Occupancy Factors" Radiation Protection Dosimetry 5, pp.203-208, 1983

Bru43 Brunauer,S. "The Adsorption of Gases and Vapors : Volume I. Physical Adsorption", Princeton University Press, 1943

Che78 Cheremisinoff,P.N. and Ellerbusch,F. "Carbon Adsorption Handbook" Ann Arbor Science Publishers Inc., 1978

Chi77 Chiou,C.T. and Reucroft,P.J. "Adsorption of Phosgene and Chloroform by Activated and Impregnated Carbons" Carbon Vol.15, pp.49-53, 1977

Coh83 Cohen,B.L. and Cohen,E.S. "Theory and Practice of Radon Monitoring with Charcoal Adsorption", Health Physics Vol.45, pp.501-508, 1983

Coh86a Cohen,B.L. and Nason,R. "A Diffusion Barrier Charcoal Adsorption Collector for Measuring Rn Concentration in Indoor Air", Health Physics Vol.50, pp.457-463, 1986

Coh86b Cohen,B.L. "Comparison of Nuclear Trak and Diffusion Barrier Charcoal Adsorption Methods for Measurement of Rn-222 Levels in Indoor Air", Health Physics Vol.50, pp.828-, 1986

Coh87 Cohen,B.L. and Gromicko,N. "Adequacy of Time Averaging with Diffusion Barrier Charcoal Adsorption Collectors for Rn-222 Measurements in Home", Health Physics Vol.54, 1987

DOE88a U.S.Department of Energy "Radon Inhaltion Studies in Animals" Radon Literature Survey Series, DOE/ER-0396, September 1988

DOE88b U.S.Department of Energy "Radon Epidemiology : A Guide to the Literature" Radon Literature Survey Series, DOE/ER-0399, December 1988

Dub60 Dubnin,M.M. "The Potential Theory of Adsorption of Gases and Vapors for Adsorbents with Energetically Nonuniform Surfaces", Cemical Review 60, pp.235-241, 1960

Fle84 Fleischer,R.L. "Theory of Passive Measurement of Radon Daughters and Working Levels by the Nuclear track Technique", Health Physics Vol.47, pp.263-270, 1984

Fre79 Freeman,G.B. and Reucroft,P.J. "Adsorption on HCN and H2O Vapor Mixtures by Activated and Impregrated Carbons", Carbon Vol.17, pp.313-316, 1979

Gan86 Gan,T.H., Mason,G.C., Wise,K.N., Whittlestone,S and Whlle,H.A. "Desorption of Rn-222 by Moisture and Heat", Health Physics Vol.50, pp.407-410, 1986

Geo77 George,A.C. and Breslin,A.J. "Measurement of Environmental Radon with Integrating Instruments", Workshop on Methods for Measuring Radiation in and around Uranium Mills, 1977

Geo84 George,A.C. "Passive, Integrated Measurement of Indoor radon Using Activated Carbon", Health Physics Vol.46, pp.867-872, 1984

Gol81 Golovoy,A. and Braslaw,J. "Adsorption of Automotive Paint Solvents on Activated Carbon : I. Equilibrium Adsorption of Single Vapors", Journal of the Air pollution Control Association Vol.31, pp.861-865, 1981

Gon86 Gonzalez,J. and Levine,S.P. "The Development and Evaluation of a Thermally-Desorbable Miniture Passive Dosimeter for the Monitoring of Organic Vapors" American Industrial Hygiene Association 47, pp.339-346, 1986

Gra84 Grant,R.J., Joyce,R.S. and Urbanic,J.E. "The Effect of Realtime Humidity on the Adsorption of Water-Immiscible Organic Vapors on Activated Carbon", Fundamentals of Adsorption, 1984

Har87 Harper,M. and Purnell,C.J. "Diffusive Sampling - A Review" American Industrial Hygiene Association 48, pp.214-218, 1987

ICRP87 The International Commission on Radiological protection "Lung Cancer Risk from Indoor Exposures to Radon Daughters", ICRP Publication 50, 1987

Jon81 Jonas,L.C., Billings,C.E. and Lilis,C "Laboratory Performance of Passive Personal Samplers for Waste Anesthetic Gas (Enflurane) Concentrations", American Industrial Hygiene Association 42, pp.104-111, 1981

Kah87 Kahn,B. and Gray,D. unpublished data at Georgia Institute of Technology, 1987

Kot88 Kotrappa,P., Dempsey,J.C., Hickery,J.R. and Stieff,L.R. "An Electret Passive Environmental Rn-222

Monitor Based on Ionization Measurement" Health Physics 54, pp.47-56, 1988

Luc88 Lucas,H.F. and Markum,F. "Radon in Air calibration Procedure : A Primary Method", Nuclear Science and Engineering : 99, pp.82-, 1988

Lug68 Lugg,G.A. "Diffusion Coefficients of Some Organic and Other Vapors in Air" Analytical Chemistry 40, pp.1072-1077, 1968

McB32 McBain,J.W. "The Sorption of Gases and Vapors by Solids", George Ritledge and Sons Ltd., England, 1932

Mon79 Montalvo,J.G. "Total Elemental Content Passive Personal Monitors", American Industrial Hygiene Association 40, pp.1046-1054, 1979

NAS80 National Academy of Science "The Effects on Populations of Exposure to Low Levels of Ionizing Radiation", report BEIR III of the Committee on the Biological Effects of Ionizing Radiations, 1980

NAS88 National Academy of Science "Health Risks of RADON and other Internally Deposited Alpha-Emmitters", report BEIR IV of the Committee on the Biological Effects of Ionizing Radiations, 1988

NEA83 Nuclear Energy Agency "Dosimetry Aspects of Exposure to Radon and Thron Daughter Products", NEA/OECD, 1983

NCRP84 National Council on Radiation Protection and Measurements "Evaluation of Occupational and Environmental Exposures to Radon and Radon Daughters in the United States", NCRP Report No.78, 1984

NCRP87 National Council on Radiation Protection and Measurements "Ionizing Radiation Exposure of the Population of the United States", NCRP Report No.92, 1987

Nel74 Nelson,G.O. and Harder,C.A. "Respirator Cartridge Efficiency Studies V. Effect of Solvent Vapor", American Industrial Hygiene Association, pp.391-410, 1974

Ner86 Nero,A.V., Schwehr,M.B., Nazaroff,W.W. and Revzan,K.L. "Distribution of Airborne Radon-222 Concentrations in U.S. Homes", Science 234, pp.992-997, 1986

Pal86 Palmes,E.D., Burton,Jr.,R.M., Ravishankar,K. and Solomon,J.J. "A Simple Mathematical Model for Diffusional Sampler Operation" American Industrial Hygiene Association 47, pp.418-420, 1986

Pri85 Prichard,H.M. and Marien,K. "A Passive Diffusion Rn-222 Sampler Based on Activated Carbon Adsorption", Health Physics Vol.48, pp.797-803, 1985

Pus88 Puskin,J.S. and Yang,Y "A Retrospective Look at Rn-Induced Lung cancer Mortality from the Viewpoint of a Relative Risk Model", Health Physics Vol.54, pp.635-643, 1988

Ros82 Rose,V.E. and Perkins,J.L. "Passive Dosimetry - State of the Art Review", American Industrial Hygiene Association 43, pp.605-621, 1982

Reu77 Reucroft,P.J. and Chiou,C.T. "Adsorption of Cyanogen Chloride and Hydrogen Cyanide by Activated and Impregnated Carbons", Carbon Vol.15, pp.285-290, 1977

Rue84 Ruecroft,P.J. "Mixed Vapor Adsorption on Activated Carbon", Fundamentals of Adsorption, 1984

Ros82 Rose,V.E. and Perkins,J.L. "Passive Dosimetry - State of the Art Review", American Industrial Hygiene Association 43, pp.605-621, 1982

Sil69 Sill,C.W. "An Integrating Air Sampling for Determination of Radon-222", Health Physics Vol.16, pp.371-, 1969

Str81 Strong,K.P. and Levins,D.M. "Dynamic Adsorption of Radon on Activated Carbon", 15th DOE Nuclear Air Cleaning Conference, pp.627-639, 1981

Tom77 Tompkins,F.C. and Goldsmith,R.L. "A New Personal Dosimeters for the Monitoring of Industrial Pollutants", American Industrial Hygiene Association 38, pp.371-377, 1977

Und77 Underhill,D.W. "Release of Adsorbed Krypton and Xenon from Spilled Charcoal", Nuclear Science and Engineering 63, pp.133-142, 1977

Und80 Underhill,D.W. and Moeller,D.W. "The Effects of Temperature, Moisture, Concentration, Pressure and Mass Transfer on the Adsorption of Krypton and Xenon on Activated Carbon", NUREG-0678, 1980

Und83 Underhill,D.W. "Unbiased Passive Sampling" American Industrial Hygiene Association 44, pp.237-239, 1983

Und84 Underhill,D.W. "Efficiency of Passive Sampling by Adsorbents", American Industrial Hygiene Association 45, pp.306-310, 1984

Und86 Underhill,D.W., DiCello,D.C., Scaglis,L.A. and Watson,J.A. "Factors Affecting the Adsorption of Xenon on

Activated carbon", Nuclear Science and Engineering 93, pp.411-414, 1986

Und87 Underhill,D.W. "Calculation of the Performance of Activated carbon at High Relative Humidities" American Industrial Hygiene Association 48, pp.909-913, 1987

UNS77 United Nations Scientific Committee on the Effects of Atomic Radiation "Sources and Effects of Ionizing Radiation", 1977

Van87 Van Den Hoed,N., Van Asselen,O.L.J. and Van Dongen,J.P.C.M. "Replicate Side-By-Side Field Comparison of 3M Diffusive Samplers Versus Charcoal Tube Samplers for Styrene" American Industrial Hygiene Association 48, pp.252-256, 1987

Wat86 Watnick,S, Latner,N and Gravenson,R.T. "A Rn-222 Monitor Using Alpha-Spectroscopy", Health Physics Vol.50, pp.645-646, 1986

Wer85 Werner,M.D. "The Effects of Relative Humidity on the Vapor Phase Adsorption of Trichloroethylene by Activated Carbon", American Industrial Hygiene Association 46,. pp.585-590, 1985

Wil86 Wilkening,M. and Wilke,A. "Seasonal Variation of Indoor Rn at Location in the Southernwestern United States", Health Physics Vol.51, pp.427-, 1986

Woo87 Wood,G.O. "A Model for Adsorption Capacities of Charcoal Beds I. Relative Humidity Effects", American Industrial Hygiene Association 48, pp.622-625, 1987

Woo87 Wood,G.O. "A Model for Adsorption Capacities of Charcoal Beds II. Challenge Concentration Effects", American Industrial Hygiene Association 48, pp.703-709, 1987

Yoo84a Yoon,Y.H. and Nelson.J.H. "Application of Gas Adsorption Kinetics I.A Theoretical Model for Respirator Cartridge Service Life", American Industrial Hygiene Association 45, pp.509-516, 1984

Yoo84b Yoon,Y.H. and Nelson,J.H. "Application of Gas Adsorption Kinetics II.A Theoretical Model for Respirator Cartridge Service Life and Its Practical Applications", American industrial Hygiene Association 45, pp.517-524, 1984